The effects of resistance training on skeletal muscle senescent cell and denervation markers in older adults

by

Bradley A. Ruple

A dissertation submitted to the Graduate Faculty of

Auburn University

in partial fulfillment of the

requirements for the Degree of

Doctor of Philosophy in Kinesiology

Auburn, Alabama

August 5, 2023

Approved by

Michael Roberts, PhD, Chair, Professor of Kinesiology

L. Bruce Gladden, PhD, Professor of Kinesiology

Austin Robinson, PhD, Associate Professor of Kinesiology

C. Brooks Mobley, Ph.D. Assistant Clinical Professor of Kinesiology, Auburn University

Abigail L. Mackey, Ph.D. Clinical Professor, Department of Clinical Medicine, University of Copenhagen

ABSTRACT

Emerging mechanisms associated with skeletal muscle aging include the increased presence of denervated myofibers and senescent cells. However, sparse research exists regarding how resistance training affects these outcomes. Thus, we sought to examine how eight weeks of unilateral leg extensor resistance training (2d/week) affected denervated myofibers, senescent stromal cells, and associated protein markers in untrained, middle-aged participants (MA, 55±8 years old, 17 females, 9 males). Vastus lateralis (VL) ultrasound images, biopsies, and strength assessments were obtained from the trained and untrained legs prior to (PRE) and following the intervention (POST). Type I/II/mixed fiber cross-sectional areas (fCSA), satellite cells (Pax7+), denervated myofibers (NCAM+), and senescent cells (p16+ or p21+) were assessed in 20 of these participants. In the trained leg of a subset of these participants, proteomics data was manually interrogated to examine proteins associated with muscle-nerve communication and senescence (n=18), and a targeted antibody-based array was used to examine senescence-associated secretory phenotype (SASP) protein expression (n=13). Leg extensor peak torque increased with training ($p<0.001$), and an interaction for muscle cross-sectional area approached significance ($p=0.082$) whereby hypertrophy favored the trained leg. While no significant interactions existed for I/II/mixed fCSAs, the percentage of NCAM+ type I/II/mixed myofibers, or senescent (p16+ or p21+) cells, a significant interaction ($p=0.037$) was evident for satellite cells whereby an increase occurred in the trained leg ($p=0.020$). Interestingly, while >90% satellite cells were not p16+ or p21+, most p16+ and p21+ cells were also Pax7+ (>90% on average) indicating that most senescent cells were satellite cells. Training altered 13/46 detected proteins related to muscle-nerve communication (all upregulated, $p<0.05$) and 10/19 proteins

related to cellular senescence (9 upregulated, $p<0.05$). Of the SASP proteins, only 1/17 markers increased with training (IGFBP-3, $p=0.031$). In conclusion, while several proteins associated with muscle-nerve communication were upregulated in MA participants with training, NCAM+ myofibers were not altered. Moreover, resistance training in MA participants increased the abundance of senescence-related proteins in skeletal muscle, albeit this did not coincide with alterations in senescent cell numbers or SASP proteins. Finally, given that p16+ or p21+ were not affected with training, we speculate that the training-induced increase in satellite cells or the proliferation of an unidentified cell type may have accounted for the increases in senescence-related proteins, and that resistance training is not a driver of cellular senescence.

ACKNOWLEDGEMENTS

I am beyond grateful for my time here at Auburn and all of the opportunities I have had. I would like to express my deepest gratitude to my advisor, Dr. Roberts, for the invaluable guidance, patience, and continuous encouragement throughout the duration of this journey. Your expertise, insightful feedback, and the environment you have created here at Auburn have played an instrumental role in shaping the direction and quality of my research. I am honored to have had the opportunity to have you as my mentor.

I am also tremendously appreciative of the members of my dissertation committee, Dr. Gladden, Dr. Mackey, Dr. Mobley, and Dr. Robinson, for your valuable insights, constructive criticism, mentorship, and suggestions which have greatly enriched this work. For your expertise in your respective fields have been instrumental in broadening my understanding and developing me into my own scientist.

I would like to extend a special thank you to my best friend, my confidant, and my greatest supporter, my wife, Mariah Ruple. Your unwavering love and support have kept me steady throughout this demanding journey. Your willingness to listen to my ideas and frustrations with constant encouragement through each triumph and challenge have been a source of strength and motivation, and I am grateful for you by my side. While our “career year” is coming to an end, I can’t wait to see what the next chapter holds.

I am indebted to both past and present MASL members, whose camaraderie, intellectual discussions, and shared experiences have made this journey enjoyable and rewarding. Dr. Kaelin Young, another day in the bonus round and I don’t think I would be in the bonus round if it

wasn't for you. Dr. Morgan Smith, while you weren't here for the study, you were always willing to listen and help in any way that you could, both in science and in life. Dr. Shelby Osburn, you took me under your wing and showed me the ropes in almost every aspect of being a great PhD student. Josh Godwin, for the opportunities to learn and grow alongside you throughout this journey. Lastly, the little siblings of the lab, Nick and Mads, thank you for the endless laughter, entertainment, and keeping me motivated.

My deepest appreciation goes to my family for their love throughout this entire endeavor. While they still think I'm going to become a physical therapist, their support and blind belief in my abilities have helped and inspired me to stay on track, and I am truly grateful for them in my life.

Lastly, I would like to express my heartfelt gratitude to all the participants and individuals who generously contributed their time to this research. Without their cooperation and willingness to participate, this study would not have been possible.

This dissertation represents the culmination of years of hard work, dedication, and the collective efforts of numerous individuals. I am truly grateful for the support and encouragement I have received along the way, and I humbly acknowledge the contributions of all those who have played a part in this academic journey.

TABLE OF CONTENTS

LIST OF TABLES

LIST OF FIGURES

LIST OF ABBREVIATIONS

NMJ	Neuromuscular junction
NCAM	Neural cell adhesion molecule
fCSA	Fiber cross-sectional area
mCSA	Muscle cross-sectional area
VL	Vastus Lateralis
p16	$p16^{INK4a}$; cyclin-dependent kinase inhibitor 2a
p21	$p21^{WAF1/CIP1}$; cyclin-dependent kinase inhibitor 1a
SASP	Senescence-associated secretory phenotype
EMG	Electromyography
ACh	Acetylcholine
AchR	ACh receptor
T-tubules	Transverse tubules
DHPR	Dihydropyridine receptor
RyR	Ryanodine receptor
PGC-1a	Peroxisome proliferator-activated receptor-γ coactivator
mTORC1	Mammalian target of rapamycin complex 1
3RM	3-repetition max
RIR	Repetitions in reserve
MHC	Myosin heavy chain
USG	Urine specific gravity assessment
$ICC_{3,1}$	Intraclass correlation coefficient
SEM	Standard error of the measurement

MD	Minimal difference
NPs	Nanoparticles
PBS	1x phosphate buffered saline
DAPI	4=,6-diamidino-2-phenylindole
Pax7	Paired box7

Chapter I: Introduction

Skeletal muscle is a tissue that is responsible for force generation, locomotion, and heat production [1]. Skeletal muscle consists of thousands of muscle fibers, or myofibers, and each fiber is innervated by a single alpha motor neuron. This neuron, and all the myofibers it innervates, is collectively termed a motor unit. Functionally, the motor neuron is responsible for sending electrical signals from the nervous system to the muscle to elicit muscle contraction. However, this muscle-nerve communication can be altered, specifically at the site of the neuromuscular junction (NMJ) [2, 3]. The NMJ exhibits plasticity, and when destabilization occurs, axonal sprouting from the motor neuron can re-establish muscle-nerve communication [4]. When a motor neuron is no longer communicating with a myofiber, this is referred to as denervation [5]. With aging there is both accelerated denervation and impaired reinnervation [6, 7]. Additionally, there is preferential denervation of type II fibers occurs, and these myofibers are re-innervated by lower-threshold motor units leading to a greater proportion of type I fibers. This phenomenon is referred to as fiber type grouping [3]. Additionally, the age-related loss in reinnervation results in myofiber atrophy. A well-established characteristic of aging is sarcopenia, or an age-related muscle loss [8]. A loss in myofiber innervation likely partially explains why age-related atrophy ensues. In this regard, neural cell adhesion molecule (NCAM)-positive myofibers (which signifies denervation) are higher in older versus younger participants, thus confirming this occurrence [9, 10].

While there have been multiple studies demonstrating the benefits of exercise for older individuals [11-15], there is limited research on denervated fibers in response to exercise; specifically, there is lack of agreement on how exercise affects NCAM-positive fibers [16-19]. Additionally, older individuals have been posited to have a blunted hypertrophic response to

resistance training, and a recent meta-analysis supported that increased myofiber hypertrophy to resistance training is inversely proportional to age [20]. These data could be explained, in part, by the presence of more denervated myofibers and/or altered NMJ characteristics in older versus younger individuals.

Another emerging cellular contribution to the diminished hypertrophic response to resistance training in older individuals is the presence of more senescent cells. p16 (INK4a; CDKN2A) and p21 (WAF1/CIP1; CDKN1a) are key markers of senescence that inhibit cyclin-dependent kinases and promote cell cycle arrest [21-23]. In general, senescent cells are defined as a cell type that lose their regenerative capacity and secrete molecules associated with inflammation (i.e., senescence-associated secretory phenotype (SASP)) [24]. Dungan and colleagues reported aging was associated with increased senescent cell abundance in muscle tissue [25]. Specifically, older mice presented more senescent cells in the extracellular matrix of the plantaris muscle in response to synergist ablation-induced mechanical overload (but not in the basal state) relative to younger adult mice and this coincided with an impairment in muscle hypertrophy. However, when older mice were administered a senolytic cocktail (i.e., dasatinib and quercetin, or D+Q), this reduced the presence of senescent cells in older mice and rescued the impaired hypertrophy phenotype. While these data are informative, little is known in older humans regarding the association between senescent cell abundance and hypertrophic responses to resistance training.

In closing, skeletal muscle and the NMJ characteristics are altered with aging, although there is little evidence to support whether possessing a greater number of denervated myofibers is associated with impaired resistance training adaptations. While rodent data support a

heightened senescent cell abundance as being a hinderance to mechanical overload-induced hypertrophic outcomes, it is unknown as to whether this phenomenon translates to humans.

Specific aims of this proposal

1. Examine whether there are basal differences in amount of denervated (NCAM+) myofibers and senescent (p16+ or p21+) cells in middle aged individuals, compared to younger college-aged individuals.
2. In older individuals, examine whether eight weeks of unilateral leg extensor resistance training (2 d/wk) decreases NCAM+ myofibers and p16+ or p21+ cells.
3. Examine whether eight weeks of training alters proteins related to muscle-nerve communication and cellular senescence, as well as comparing older participant data from the trained leg to the younger adult comparator group.
4. Lastly, determine whether the alterations in denervation or senescent cells are associated with corresponding changes in hypertrophy.

Hypotheses

1. Older participants will possess more denervated myofibers and senescent cells compared to college-aged participants in the basal state.
2. In older participants, resistance training will lower the number of denervated myofibers and associated proteins in the training leg, while the non-training leg will exhibit no changes in these outcomes.
3. Senescent cell abundance, and proteins associated with cellular senescence, will increase in the trained leg of middle-aged participants, and this will occur more so in those that are older (e.g., > 60 years of age) versus those that are younger (e.g., < 45 years of age).

4. There will be a significant inverse correlation between the senescent cell response and hypertrophic response in the trained leg of older participants.

Chapter II: Literature Review

Skeletal Muscle

Skeletal muscle is one of the most dynamic tissues of the human body. It accounts for about 40% of an individual's body mass and facilitates locomotion, substrate metabolism, and heat production. Muscle is encapsulated with multiple layers of connective tissue. First, the epimysium surrounds the entire muscle. Next, perimysium surrounds bundles of muscle fibers, often referred to as fascicles. Lastly there is the endomysium, which surrounds individual muscle fibers. Muscle fibers (synonymous with muscle cells or myofibers) possess similar organelles as other cells but also contain unique cell-specific organelles. Muscle fibers are long and cylindrical, and are classified as post-mitotic, meaning the cell can no longer divide via mitosis. Another unique property of myofibers is that they are one of the few cell types in mammals that are multi-nucleated. The myonuclear domain theory posits each nucleus is responsible for a given sarcoplasmic space in the myofiber [26]. Satellite cells, or muscle stem cells, exist near myofibers between the basement membrane and the sarcolemma [27]. Satellite cells play a major role in muscle growth, damage, and repair [28]. In mature muscle fibers, satellite cells are usually quiescent, but upon damage or trauma, become activated. In response to mechanical overload, satellite cells differentiate into myoblasts to donate their nucleus to the muscle fiber [29]. However, several aspects of satellite cells are still debated, such as whether satellite cell-mediated myonuclear accretion is needed for myofiber growth in adulthood [30] or whether satellite cell numbers [31-34] or function decline with age [34-38].

Sarcomeres, the functional unit of myofibers, consist of numerous contractile proteins that are also responsible for muscle's striated appearance. Sarcomeres are oriented in series to form myofibrils. Two of the most abundant proteins, actin (thin filaments) and myosin (thick

filaments), form cross-bridges to produce a muscle contraction. Myosin is a unique protein that is highly expressed in myofibers and contains several domains which contribute to its function as a molecular motor [39]. The three structural domains of myosin include the head, neck, and tail. The head domain is especially relevant to muscle contraction given that it possesses ATPase activity to harness cellular energy and a sequence of conserved amino acids that exhibit a high binding affinity to actin monomers [40]. Other organelles that surround myofibrils include the sarcoplasmic reticulum and mitochondrial reticulum [41]. The sarcoplasmic reticulum is responsible for the storage, release, and reuptake of calcium. When calcium is released into the sarcoplasm it binds to troponin C on the actin myofilament, causing a conformational change of tropomyosin, exposing the actin-myosin binding site. These events allow for myosin to bind to actin, creating the cross-bridge formation. The mitochondria are primarily responsible for producing cellular energy, specifically adenosine triphosphate or ATP. ATP is needed to provide energy for conformational changes to the neck of the myosin protein (i.e., the power stroke), which leads to the shortening of sarcomeres and the generation of force. Myosin will stay bound to actin until ATP is reattached. Once attached, the myosin head is detached from actin, ATP is hydrolyzed into ADP and Pi, returning myosin into the energized position. The enzymatic rate of a particular ATPase isozyme reflects the myosin heavy chain isoform [42].

Beyond contractile properties, myofibers possess different biochemical properties. These characteristics include, but are not limited to, volume of mitochondria, amount of myoglobin, and the content and kinetics of enzymes in the various energy systems. Based on these characteristics, as well as the predominant myosin protein expressed muscle fibers are characterized into either slow (type I) or fast (type II) fibers. The type II fiber can be further subdivided into two sub-types, IIa (intermediate) and IIx (fast) [43]. Compared to type II fibers,

type I fibers contain more mitochondria, and have a greater concentration of myoglobin, making them fatigue-resistant and suitable for aerobic metabolism. Type II fibers possess relatively lower amounts of mitochondria and myoglobin and are more reliant on anaerobic metabolism for ATP production leading to both their glycolytic properties and increased fatiguability. Contractile properties also distinguish muscle fiber types. Per cross-sectional area, type II fibers have a greater concentration of actin and myosin filaments, allowing for more cross-bridges to form during muscle contraction. In addition, the V_{max} of myosin ATPase is greater in type II fibers allowing for a higher contraction velocity.

Although there is some evidence to suggest fiber type plasticity is somewhat limited over shorter terms of exercise training, a person's fiber type make-up is not fixed. Fiber type shifting can occur depending on the muscle [44], longer-term exercise training [45, 46], or age [47, 48]. There is also evidence that fiber type distribution exists in more of a continuum, allowing for "hybrids" of type I/IIa or IIa/IIx, and anywhere in between [43, 49]. With endurance training, type II fibers become more oxidative (i.e., increased mitochondrial density and function) [50], while resistance training promotes alterations in contractile properties (i.e., increase contractile proteins, force, power, etc.) and type II fiber shifting (i.e., IIx to IIa) [51, 52].

Physiology of Muscle Activation or Muscle-Nerve Communication

Besides histochemical profiling or gel electrophoresis of muscle fibers, another manner used to identify fiber type includes the utilization of electromyography (EMG) methods to profile motor unit characteristics. A motor unit is a single alpha motor neuron and all the myofibers it innervates. There are an estimated 35,000 motor neurons in the upper limbs [53] and

approximately 60,000 motor neurons in the lower limbs [54]. Each motor neuron can innervate hundreds to thousands of fibers, depending on the muscle [55, 56].

Early work by Robert Burke categorized motor units by different properties such as contraction speed and fatiguability [57, 58]. This classification system delineated three distinct motor unit types including: i) fast fatigue, matched with type IIx myofibers, ii) fatigue-resistant fibers, matched with type IIa myofibers, and iii) slow/slow twitch, matched with type I myofibers. Motor neurons innervate myofibers with similar metabolic and contractile characteristics [59]. Functionally, the motor unit provides output for the central nervous system, converting neural signals from the primary motor cortex into force that generates movement. The convergence of muscle-nerve communication occurs at the neuromuscular junction (NMJ). At the end of the neuron (i.e., the presynaptic membrane) exists synaptic vesicles which contain the acetylcholine (ACh) neurotransmitter. On the motor end plate of the sarcolemma (i.e., the postsynaptic membrane) are ACh receptors (AchRs). AchRs are located within folds near voltage-gated sodium channels to initiate the muscle action potential. When an action potential arrives at the nerve terminal, exocytosis of the synaptic vesicles occurs thereby releasing ACh into the synaptic cleft. ACh binds to the AchR causing an influx of sodium into the muscle fiber resulting in the depolarization (i.e., an end plate potential). Following end plate depolarization, an action potential traverses across the sarcolemma and down the transverse tubules (T-tubules). On the invagination of the T-tubules exists a voltage-sensor receptor termed the dihydropyridine receptor (DHPR). When the action potential reaches the DHPR, it signals the ryanodine receptor (RyR) on the lateral sac of the sarcoplasmic reticulum to release calcium into the sarcoplasm. Cross-bridge cycling subsequently occurs through the interaction of myosin and action, as discussed in the previous section.

The NMJ can adapt to various stressors [60]. For example, impaired transmission from disuse (i.e., aging, inactivity, disease) can result in axonal sprouting, or the formation of a new NMJ site [4]. If this maintenance of the NMJ did not occur, this would lead to a permanently denervated muscle fiber. Soendenbroe et al. [5] described bidirectional signaling between myofiber and the motor neuron to maintain NMJ plasticity. Briefly, anterograde signaling is the motor neuron signaling to muscle fibers allowing for the maintenance of normally functioning muscle cells. Retrograde signaling refers to the transport of molecular signals to the motor neuron from the muscle. The latter is just as beneficial as anterograde signaling because muscle cells can communicate with the nerve to maintain a normally functioning NMJ [61]. For example, a study showed an overexpression of PGC-1α, an enzyme characteristically high in type I fibers, promoted the motor neuron to a slower twitch phenotype [62]. If either bidirectional signal is diminished (from inactivity, injury, or disease), this would lead to atrophy due to either neuromuscular junction destabilization or denervation [63].

Skeletal Muscle with Aging

Muscle mass decreases with age, which begins around the fourth decade of life in men and women [48, 64]. Age-related skeletal muscle atrophy involves a reduction in muscle fiber size [65]. Both type I and type II fibers atrophy, but type II fibers typically exhibit greater age-related atrophy [66-68]. While strength peaks at ~35-to-45 years old in men and ~30-to-50 years old in women [69], age-related decrements in muscle mass are accompanied by a decrease in strength [70]. Frontera et al. [71] performed a 12-year longitudinal study in 12 men (initial average age = 65 years old) and reported that elbow and knee flexor and extensor muscle atrophy (~12-16%) and strength decrements (~20-30%) occurred simultaneously. Kemmler et al. [72]

reported that leg extensor and flexion strength also exhibit age-related decrements. Muscular power has also been reported to decrease with aging, and this age-associated malady has been associated with functional performance decrements [73]. For instance, Reid et al. [74] performed a three-year longitudinal study in older adults and reported that leg power (but not strength) decreased in an age-related fashion. Skelton et al. [75] reported similar findings whereby knee extensor peak power (but not strength) decreased in an age-related fashion. Age-related decrements in strength and power are likely due to the reduction in type II fiber number and size with aging [76]. Moreover, a destabilization of the NMJ occurs with aging [2, 3, 77, 78], and this outcome could lead to the loss and atrophy of type II myofibers. Finally, age-related decrements in power could be attributed to an age-associated loss of myosin content within muscle fibers [79], leading to decreased cross-bridge interactions [80].

Several lines of evidence support neural and neuromuscular deficits are evident in older adults. For instance, cadavers from individuals above the age of 60 years old possess less lumbospinal motor neurons [54]. A separate study indicated that the total number of vastus lateralis motor units (estimated using EMG) was ~70% lower in older versus younger adult men [81]. With aging there is a consistent cycling of myofiber denervation and reinnervation [82]. Further, there are several studies to suggest that type II fiber denervation preferentially occurs, and these fibers are subsequently reinnervated by type I motor neurons [3, 43, 83]. This phenomenon, referred to as type I fiber grouping, leads to an increased proportion of type I fibers in aged muscle [77], and consequently leads to older individuals presenting considerably lower motor unit number estimates and a loss in type II muscle fibers compared with younger individuals [48, 78, 84-86].

Satellite cell abundance and myonuclear number can also be affected by aging, albeit there is a lack of agreement with how aging affects their content. With aging, investigators have reported either no change in myonuclear number [37, 87], an increase [34, 88], or only a decrease in type II fiber myonuclei occurs [33]. Also notable, the changes in myonuclei with aging may be inversely proportional to the changes in satellite cell abundance. In two studies that reported myonuclear number per myofiber increases with age [34, 88], satellite cell abundance was concomitantly decreased. Notwithstanding, the data on satellite cell content changes with aging are also equivocal, with some research groups reporting either no change [33, 37, 89] or a decrease [31, 32, 34]. Also notable, satellite cell function also seems to be impaired with aging. Schultz and Lipton [90] investigated the proliferative capacity of satellite cells with donor age and reported an inversely proportional relation. This is further emphasized by the work of Sousa-Victor et al. [35] showing that satellite cells can enter a senescent state where they fail to proliferate upon stimulation. These findings demonstrate that satellite cells may have a limited number of replicative cycles and that a loss in function with "exhaustive proliferation" potentially limits their role in muscle growth and repair [91].

Cellular Senescence

Another cellular response found that increases with age is cellular senescence [92], or the permanent state of cell cycle arrest [93]. Hayflick and Moorhead [94] first reported the presence of cellular senescence by demonstrating that human diploid fibroblasts presented a finite capacity to divide in culture. Since this foundational report, there has been an intense research interest surrounding the consequences of cellular senescence. Senescence typically occurs in response to cell stressors that lead to the increase in DNA damage and in response to telomere shortening

[95-97]. While senescent cells can no longer divide, they remain metabolically active and secrete pro-inflammatory factors; this being termed as a senescence-associated secretory phenotype (SASP). Secreted SASP markers are abundant, potentially cell- or tissue-specific, and include proteins such as growth/differentiation factor 15 (GDF15), stanniocalcin 1 (STC1), serine protease inhibitors (SERPINs), matrix metalloproteases, and various chemokines (e.g., CXCL5, CCL3) [98].

Although senescent cells secreting SASP-associated factors may have beneficial effects [99], these cells are commonly associated with detrimental consequences [100, 101]. Senescence can also occur in post-mitotic cells [102-104], and senescence plays a role in remodeling, injury, cancer, and aging [105-108]. There are age-associated transcripts that are implicated in cellular senescence [109] and an increase in senescent cells can affect gene expression by downregulating growth stimulatory genes and increasing the expression of growth inhibitory genes [110]. Senolytic agents (e.g., Dasatinib, Quercetin, Fisetin and Navitoclax) can significantly reduce senescent cells and have garnered attention as potential treatments for age-related diseases [111]. Further, it has been reported that health and lifespan increased in mice when senescent cell abundance was reduced through the administration of senolytic agents [112].

Dungan et al. [113] reported that the experimental induction of skeletal muscle injury increases senescent cell abundance in younger and older mice. However, senescent cells remained elevated in older mice, and this was associated with an impairment in muscle regeneration. Dungan et al. [25] performed a follow-up study investigating if senescent cells affected the hypertrophic response to synergist ablation in mice. Older mice accrued more senescent cells after mechanical overload and this coincided with a blunted hypertrophic response [25]. Additionally, when a senolytic agent was administered to older mice, senescent

cells decreased and both muscle mass and fCSA increased accordingly [25]. However, whether or not senolytics resulted in a reduction in secreted SASP phenotype markers was not examined and requires further interrogation.

Skeletal Muscle Denervation

Denervation refers to the loss of the motor neuron innervating a muscle fiber. Denervated muscles can become reinnervation by nearby axonal sprouting [4, 114], but denervation can become permanent when there is a reduced retrograde stimulus from the denervated fiber, which would limit axonal sprouting following denervation [6, 115]. Myofibers undergoing acute or chronic denervation can develop morphological changes. For instance, in aged rodent models there is a loss in pre-synaptic vesicles [116] and nerve terminals [116], a reduction in the area of motor endplates [117], a decrease in acetylcholine receptors [118], and a decrease in junctional folding [119, 120]. Additionally, there are several denervation-related transcripts that are associated with aging, indicating the loss of the muscle-nerve connection. Examples include neural cell adhesion molecule (NCAM) [121-124], F-box proteins [125], AChR subunits [6, 121, 126], cytoplasmic phospholipase A2 [127], sodium channel $Nav_{1.5}$ [128, 129] and developmental myosin [121, 130].

NCAM is an immunoglobulin molecule and is part of an adhesion-mediated signaling pathway involved in cell/cell adhesion and recognition [131]. NCAM can be found in developing muscles to help attract motor neurons to regulate the myofiber innervation, but after development, NCAM is almost undetectable with myofibers [5, 132-134]. Interestingly, NCAM has been proposed to be highly expressed in denervated skeletal muscle [133, 135, 136] or

during NMJ destabilization [136, 137]. With denervation, myofibers have been posited to upregulate NCAM to interact with adjacent NCAM on axons due to homophilic interactions [138, 139]. This is supported by the expression of NCAM following denervation being detected as early as two days and remains elevated up to 300 days with denervation [136, 140]. Upon reinnervation, NCAM becomes downregulated as shown with NCAM becoming nearly absent two weeks after nerve crush, a technique shown to facilitate reinnervation [136, 141]. Unfortunately, this was in animal models, so there is a lack of a time course data of these events in human participants. Notwithstanding, the presence of NCAM+ myofibers has also been reported in paralyzed participants or in conditions whereby there is an increased presence of denervated fibers (i.e., myopathy) [132, 136]. Since aging is associated with an increase in denervation, it is not surprising that researchers have reported increased NCAM expression in the skeletal muscle of older participants [121, 122, 124, 142]. What is surprising, however, is the potential age-associated inability to upregulate NCAM upon denervation [143], which may be a driving component in the inability of myofibers to undergo reinnervation with advanced aging.

AChR is an integral membrane glycoprotein tightly associated with the lipid bilayer of the sarcolemma. Its role is to facilitate neuromuscular activity via ACh ligand binding, ultimately leading to the voluntary contraction of myofibers. There are five primary subunits of the AChR (α, β, ε, γ, and δ), and it has been reported that all subunits are upregulated (except the ε-subunit) with NMJ instability in mice [63]. AChRs are primarily located at the end plate of the NMJ [144, 145], but in denervated muscle can be found on extra-synaptic regions [126, 146]. When a muscle becomes denervated, the myogenin protein becomes highly induced [147], and a dysregulation in AChRs has been linked to elevated levels of multiple myogenic regulatory factors [144, 148, 149]. This response is likely due to myogenic regulatory factors acting *in trans*

to affect the expression of AChR genes as a compensatory response to establish reinnervation [150-152]. Denervation in chickens increases mRNA for the AChR α subunit [153], as well as the transcriptional activity of AChR genes (α, δ, and γ) as early as 9 hours after denervation [154]. Similar findings have been reported in other animals, with denervation inducing the increase in α, β, γ, and δ AChR subunit mRNA levels [146, 155, 156]. As stated earlier, AChR can be localized to extra-synaptic regions with denervation [126, 146] thereby requiring less ACh to produce muscle contraction (i.e., increased sensitivity) [126, 157]. Given that aging is associated with increased denervation, AChR content would be expected to be impacted. However, conflicting data have been reported in humans. For instance, Sonjak et al. reported AChR α, ε, and γ did not show any differences between age groups [10], while others have shown AChR α expression to be higher with age [83]. Two other groups reported different results regarding AChR γ mRNA levels with age [9, 121]. Notably, it is challenging to histologically assess AChR from human biopsies given the small amount of muscle tissue as well as the scarcity of NMJs captured through the muscle biopsy technique. Hence, more refined approaches are needed in this area to add further clarity.

Resistance training adaptations in younger versus older participants

Resistance training can mitigate or reverse specific aging-related factors in skeletal muscle [158-160]. For instance, resistance training can slow the progression of age-related muscle atrophy and functional decrements [161-164]. Moreover, Aagaard et al. [76] reported that lifelong exercise training results in greater muscular strength (both endurance and resistance trained compared to untrained), and that older resistance-trained individuals present greater myofiber size values compared to untrained and lifelong endurance-trained participants. Despite

these compelling data, some reports indicate that overload induced skeletal muscle hypertrophy is impaired in older participants [164-166], while others show aging does not affect this training adaptation [167-169]. Although this area of research is mixed, a recent meta-analysis supported that a blunted hypertrophic response in type I and II fibers with training is negatively associated with age [20]. One of the likely mechanistic causes of age-associated decreased muscle plasticity to resistance training is the change in protein metabolism with age and the response with exercise. The mammalian target of rapamycin complex 1 (mTORC1) signaling pathway is the hub for promoting protein synthesis [170]. With training, mTORC1 signaling is upregulated and is responsible for translation initiation, elongation, and overall is crucial for muscle hypertrophy [171]. It has been reported that mTORC1 signaling pathway activation is reduced with age in response to training [172]. Furthermore, older participants have a blunted muscle protein synthesis response at rest [173-176], postprandially [177, 178], and following resistance training interventions [173, 179]. Older individuals also present a reduction in the number of transcriptionally active genes in skeletal muscle in response to resistance training [180]. This phenomenon could be due, in large part, to the methylation status of genomic DNA. Voisin et al. [181] reported numerous genes responsible for muscle structure and development to be differentially methylated with age. Notably, increased methylation reduces the ability of a gene to be transcriptionally active [182]. However, with exercise, the genome-wide methylation changes have been reported to occur [183-185], and this too may be an involved mechanism in the “rejuvenating” effects of resistance training on muscle form and function.

Regardless of impaired hypertrophic outcomes with aging, resistance training has been shown to promote increases in strength in older individuals [167, 186-188]. Under this pretense, it is likely that neural adaptations are the main contributor to training-induced outcome. Indeed,

Barry et al. [189] reported that after a four-week resistance training period, torque development and EMG parameters increased similarly between younger and older participants. This finding could be due to increased motor unit firing rates and recruitment patterns during muscle contractions. In addition, Kamen and Knight [190] reported similar increases in strength after six weeks of resistance training in younger and older participants. Further, the authors reported an increase in maximal motor unit discharge rate in both age groups [190]. Lastly, Power et al. [191] investigated motor unit number estimation in well-trained runners, an elderly aged-matched group, and a young recreationally active group. While the older runners displayed lower strength, they had a greater motor unit number estimation value compared to the aged-match group and these values were similar to the younger cohort [191]. All these studies support that exercise training (and resistance training in particular) maintains various aspects of muscle-nerve communication.

Finally, while it is well established that there are multiple benefits of exercise with maintaining muscle quality with aging, there are few investigations into determining whether exercise reduces denervated myofiber abundance in older participants. Messi et al. [17] reported that a five-month resistance training program reduced both percent area of NCAM+ muscle fibers and NCAM-related gene transcripts in a relatively small sample size of older participants. Brightwell et al. [19] reported that six months of aerobic training did not statistically alter the amount of NCAM-positive muscle fibers, and again this was a relatively small sample size. Voigt et al. [16] reported similar findings in seven elderly participants with 14 weeks of resistance training. Lastly, Soendenbroe et al. [18] recently published a 16-week resistance training study examining multiple markers of denervation and reported no change in NCAM-

positive muscle fibers after following the intervention. Notwithstanding, and given the overall lack of and conflicting data, more research in this area is needed.

Purpose Statement

As stated above, aging is associated with a loss of muscle mass. Myofibers undergo cycles of denervation and reinnervation during aging, and eventually reinnervation discontinues leading to myofiber atrophy and a loss in muscle mass. Many studies examining indicators of denervation with exercise training have examined older participants (>65 years old) and compared them with young participants (<30 years old). However, these data in middle-aged participants are lacking. Finally, while evidence in rodents exists, no study to our knowledge has examined how aging and/or resistance training affects senescent cell abundance, and this too may be a factor in the reduced plasticity of muscle during periods of resistance training. Therefore, the purpose of this study is multifaceted. First, we sought to elucidate denervation markers in a middle-aged population (40-65 years old) before and after eight weeks of unilateral leg extensor resistance training. Our second aim was to investigate senescent cell abundance prior to and following the resistance training program. Third, we sought to determine how resistance training affected proteins associated with both processes as identified through a novel deep proteomics approach. Finally, we sought to compare these outcomes to tissue obtained from a college-aged cohort, which was used as a comparator group. Herein, 26 untrained, middle-aged participants completed the eight-week unilateral resistance training protocol, and muscle tissue has been collected. The following testing was performed prior to and after training in older individuals to track resistance exercise adaptations: i) bioelectrical impedance analysis for whole-body composition changes, ii) ultrasound derived right and left VL muscle cross-sectional

area, iii) peak knee extensor torque captured using an isokinetic dynamometer, iv) estimated one-repetition-max for the leg extensor exercise, and v) the donation of skeletal muscle biopsies from both legs. Middle-aged particiapnts were chosen because, based on the discussed literature, this portion of life cycle is when the denervation-reinnervation cycles could be the most accelerated. Lastly, since we implemented a unilateral training study, the non-training leg was used as a control condition to track these changes over time for all variables.

Based on the current literature the hypotheses are as follows: i) there will be a significant correlation between age and NCAM-positive fibers prior to resistance training, ii) resistance training will reduce the number of NCAM-positive fibers in the trained leg, iii) individuals showing the least reduction in NCAM-positive muscle fibers with resistance training will present impaired plasticity with other variables (e.g., less myofiber hypertrophy and strength changes), iii) senescent cell number will be upregulated with training, and a significant correlation will exist between age and the senescent cell response to training, and v) there will be a significant inverse correlation between the senescent cell response and myofiber (or whole muscle) hypertrophic response in the trained leg. No *a priori* hypothesis was developed for proteomic outcomes given that this was a secondary aim of the study, and we were unsure as to which protein targets related to phenotype outcomes would be unveiled.

Chapter III: Methods

Ethical approval and Pre-screening

This study was a secondary investigation from multiple studies that had all procedures approved by the Institutional Review Board at Auburn University. The first protocol (Protocol #21-461 MR 2110) involved investigating the effects of unilateral leg resistance training with daily NAD3 supplementation (312 mg of combined Wasabia japonica extract, theacrine, and copper (I) niacin chelate) or a placebo in adults 40-70 years of age. Notably, the supplement ingredients reduce LDL cholesterol levels and affect sirtuin activity and NAD^+ concentrations in nucleated blood cells, and we had no reason to believe that they would affect the outcome variables of interest herein. However, to ensure this was the case, we examined the placebo and NAD3 supplementation groups for pre-to-post intervention phenotype and histology change scores. No significant differences in these scores were observed between supplementation groups for the following variables in the training leg: vastus lateralis (VL) muscle cross-sectional area (mCSA) ($p=0.693$), mixed fiber cross-sectional area (fCSA) ($p=0.187$), type II fCSA ($p=0.426$), the percentage of NCAM+ myofibers ($p=0.803$), satellite cell number ($p=0.131$), or p21+/Pax7+ cell counts ($p=0.360$), or p16+/Pax7+ cell counts ($p=0.376$). Of the 66 targeted proteins from the proteomic analysis, only one was affected with supplementation (MTR, related to "axon regeneration", was downregulated, $p=0.043$, respectively). Thus, 9 MA males and 17 MA, perimenopausal women from both supplementation groups were pooled to examine how training affected phenotype outcomes (n=26 in the trained and non-trained leg), histological outcomes (n=20 in the trained and non-trained leg), 65/66 targeted proteins from the proteome analysis (n=18 in the trained leg only, with MTR excluded from analysis).

The next two studies (Protocol #19–249 MR 1907 and #20–136 MR 2004) investigated the effects of daily peanut protein supplementation and how contractile protein and mitochondrial content adapted with 10 weeks of resistance training in adults 18-30 years of age [192, 193]. However, for the 15 participants included, only their pre-intervention characteristics were used as a comparator dataset to compare to the older participants to determine if resistance training altered muscle characteristics to "youth-like" levels. Eleven of these 15 younger participants were used for the immunohistochemical comparisons, and 9 of the 15 were used for the proteomic comparisons.

Inclusion criteria for all studies indicated that participants had to possess a body mass index <34 kg/m^2, have no or minimal experience with resistance training (≤1 day/week) over the last year, and be free of any medical condition that would contradict participating in an exercise program or donating skeletal muscle biopsies. Participants provided verbal and written consent to participate prior to data collection and the study conformed to standards set by the latest revision of the Declaration of Helsinki with the exception of being registered as a clinical trial.

Study Design

The resistance training intervention consisted of supervised unilateral leg extensions, twice per week, for eight weeks. All participants trained their right legs, with the left leg serving as a within-participant, untrained control. For each training day participants performed 5 sets of 12 repetitions per session. The beginning training load was established at ~40% of the participants 3RM (described later). After each set, participants verbally articulated their perceived repetitions in reserve (RIR), and training load was adjusted accordingly. RIR values of 0-2 after a set resulted in no training load change in each session. RIR values of 3-5 for consecutive sets resulted in the training load being increased by 5-10%. For RIR values ≥6 after

one set, the training load was increased by 10-20%. If the weight could not be performed with full range of motion, or the participant could not complete 12 repetitions for a given set, the training load was decreased.

Strength testing

The first and last workout of the eight-week training paradigm consisted of maximal leg extensor-flexion torque assessments using isokinetic dynamometry (Biodex System 4; Biodex Medical Systems, Inc., Shirly, NY, USA) and 3RM leg extensor strength testing. Notably, both legs were tested for these outcomes. Prior to dynamometer testing, the participant's lateral epicondyle was aligned with the axis of the dynamometer's lever arm, and the hip was positioned at 90°. The starting leg was randomized for everyone prior to each test. The participant's shoulders, hips, and leg were strapped and secured for isolation during testing. Following three warm-up trials at a submaximal effort, participants completed five maximal voluntary isokinetic knee extension and flexion actions at 60 degrees/second. Participants were provided verbal encouragement during each contraction. The isokinetic contraction resulting in the greatest peak torque value was used for analyses. Participants were given a one-minute rest and then the contralateral leg completed this exact protocol. Approximately five minutes following isokinetic dynamometry testing, participants performed 3RM strength testing on both the right and left leg. Prior to testing, participants were given a warm-up load and instructed to complete 10 repetitions. After participants recorded their RIR for the warmup set, the weight was adjusted accordingly for another warm-up set of five repetitions. RIR was recorded again to determine the participants starting load for a 3RM attempt. The load was incrementally increased 5-10% per 3RM attempt until 3RM testing concluded, indicated by failure of full range of motion on any of the repetitions, or if RIR recorded was 0. Participants were allowed a full three minutes of

recovery between attempts. The isokinetic dynamometry and 3RM testing described herein was similar for both the first and final workout.

Testing Sessions

Urine specific gravity testing for hydration. Participants performed a testing battery prior to the start of training (PRE) and 3-5 days following the last resistance training workout (POST). Participants arrived for testing at a minimum of four hours fasted and well hydrated. Upon arrival participants submitted a urine sample (~5 mL) for urine specific gravity assessment (USG). Measurements were performed using a handheld refractometer (ATAGO; Bellevue, WA, USA). USG levels in all participants were ≤ 1.020, indicating sufficient hydration [194].

Body composition testing. Once adequate hydration was determined, body composition was assessed using multi-frequency bioelectrical impedance analysis (InBody 520, Biospace, Inc. Seoul, Korea). From the scan, body fat percentage was recorded. Previously determined test-retest reliability on 8 participants measured twice within 24h yielded an intraclass correlation coefficient ($ICC_{3,1}$) of 0.99, standard error of the measurement (SEM) of 0.87%, and minimal difference (MD) of 1.71% for body fat percentage.

Ultrasonography assessment for muscle morphology. A detailed description of VL assessments using ultrasonography has been published previously by Ruple et al. [195]. Briefly, real-time B-mode ultrasonography (NextGen LOGIQe R8, GE Healthcare; Chicago, IL, USA) using a multifrequency linear-array transducer (L4-12T, 4–12 MHz, GE Healthcare) was used to capture right and left leg images to determine VL mCSA. Prior to scans, the mid-thigh of the leg was determined by measuring the total distance from the mid-inguinal crease in a straight line to the proximal patella, with the knee and hip flexed at 90°, a mark was made using a permanent

marker at 50% of the total length. From that location, a permanent marker was used transversely to mark the mid-belly of the VL. This marking is where all PRE ultrasound images were taken as well as the muscle biopsy (described below). POST images were taken at the PRE biopsy scar to ensure location consistency between scans. For VL mCSA, a flexible, semirigid pad was placed around the thigh and secured with an adjustable strap to allow the probe to move in the transverse plane. Using the panoramic function of the device (LogicView, GE Healthcare), images were captured starting at the lateral aspect of the VL and moving medially until rectus femoris was visualized, crossing the marked location. All ultrasound settings were held constant across participants and laboratory visits (frequency: 10 MHz, gain: 50 dB, dynamic range: 75), and scan depth was noted and held constant across time points per participant. Images were downloaded and analyzed offline using ImageJ software (National Institutes of Health, Bethesda, MD, USA). All ultrasound images were captured and analyzed by the same investigators at each timepoint. Previously determined test-retest reliability on 10 participants measured twice within 24 h (where BAR captured images and JSG analyzed images) yielded an ICC of 0.96 and 0.99, SEM of 0.09 cm and 0.60 cm^2, and MD of 0.24 cm and 1.65 cm^2 for VL thickness and VL mCSA, respectively.

Collection of muscle tissue. Muscle biopsies were obtained at PRE and POST, from the mid-belly of both the right and left VL, with sampling time of day at PRE and POST being standardized for each participant. Lidocaine (1%, 1.0 mL) was injected subcutaneously above the skeletal muscle fascia at the previously marked location. After five minutes of allowing the anesthetic to take effect, a small pilot incision was made using a sterile Surgical Blade No. 11 (AD Surgical; Sunnyvale, CA, USA), and the 5-gague biopsy needle was inserted into the pilot incision ~1 cm below the fascia. Approximately 50–80 mg of skeletal muscle was removed

using a double chop method and applied suction. Following biopsies, tissue was rapidly teased of blood and connective tissue. A portion of the tissue (~10–20 mg) was preserved in freezing media for histology (OCT; Tissue-Tek, Sakura Finetek Inc; Torrence, CA, USA), slowly frozen in liquid nitrogen-cooled isopentane, and subsequently stored at −80°C until histological analysis. Another portion of the tissue (~30–50mg) was placed in pre-labeled foils, flash frozen in liquid nitrogen, and subsequently stored at −80°C until other assays described below.

Proteomics

Sample Preparation. Sarcoplasmic protein isolation for all samples occurred at Auburn University using previously described methods [196]. Approximately 30mg of tissue was homogenized using tight-fitting pestles in 500µL of 25 mM Tris, pH 7.2, 0.5% Triton X-100 (with added protease inhibitor cocktail at a 1:50 dilution; Promega, cat# G6521). Samples were then centrifuged at 1500g for 10 minutes at 4°C and the sarcoplasmic fraction supernatants were collected. 300µL of the resultant sarcoplasmic supernatants from the trained leg of 18 older participants at PRE and POST and 9 younger adult samples were used for proteomics.

Deep proteomics of the sarcoplasmic fraction was performed at Seer, Inc. (Redwood City, CA, USA). For each assay sample, 250 µL was transferred to a Seer sample tube and the standard Proteograph assay protocol was performed. After the samples were loaded onto the SP100 automation instrument, samples underwent protein corona formation and processing to purified peptides. To form the protein corona, Seer's proprietary nanoparticles (NPs) were mixed with the sarcoplasmic fractions, and incubated at 37°C for 1 hr. Unbound proteins were removed prior to downstream washing, reduction, alkylation, and protein digestion steps which are performed according to Seer's Proteograph Assay protocol [197].

LC-MS configuration. Peptides were reconstituted according to individual well peptide yield in a solution of 0.1% formic acid and 3% acetonitrile [198] spiked with 5 fmol µL PepCalMix from SCIEX (Framingham, MA, USA). Reconstitution volumes varied across NPs to allow for constant mass MS injection between samples regardless of starting volume (240ng: NP1, 400ng: NP2, 360ng: NP3, 120ng: NP4, and 320ng: NP5). 4 µl of each sample was analyzed with a Ultimate3000 RLSCnano LC system coupled with a Thermo Fisher Orbitrap Fusion Lumos mass spectrometer. First, the peptides were loaded on an Acclaim PepMap 100 C18 (0.3 mm ID × 5 mm) trap column and then separated on a 50 cm µPAC analytical column (PharmaFluidics, Belgium) at a flow rate of 1 µL min^{-1} using a gradient of 5–25% solvent B (100% ACN) mixed into solvent A (100% water) over 26 minutes. The mass spectrometer was operated in DIA mode using 10 m/z isolation windows from 380-1200 m/z and 3s cycle time. MS1 scans were acquired at 60k resolution and MS2 at 30k resolution.

Data Processing. DIA data were processed using Proteograph^{TM} Analysis Suite 2.1. Raw MS data were processed using the DIA-NN search engine (version 1.8.1) in library-free mode searching MS/MS spectra against an in silico predicted library based on Uniprot's Homo Sapiens reference database (UP000005640_9606, download December 9th, 2022). Library-free search parameters included trypsin, one missed cleavage, N-terminal Met excision, fixed modification of Cys carbamidomethylation, peptide length of 7-30 amino acids, precursor range of 300-1800 m/z, and fragment ion range of 200-1800 m/z. Heuristic protein inference was enabled, MS1 and MS2 mass accuracy was set to 10 ppm. Precursor FDR was set to 0.01, and PG q-value was set to 0.01. Quantification was performed on summed abundances of all unique peptides considering only precursors passing the q-value cutoff. PAS summarizes all nanoparticle values for a single protein into a single quantitative value. Specifically, a single protein may have been measured up

to five times, once for each nanoparticle. To derive the single measurement value, PAS uses a maximum representation approach, whereby the single quantification value for a particular peptide or protein group represents the quantitation value of the NP most frequently measured across all samples. The relative abundances of protein targets were obtained by normalizing raw spectral values to total spectra. After normalization, for proteins that were not detected, values were set at zero with the assumption the protein was in low abundance or not detected. Lastly, protein values are expressed in $\log_{10}$ values in all figures and results.

An *a priori* search was performed to filter the number of proteins used for the current analysis. Specifically, Gene Ontology (GO; http://geneontology.org, [199]) and UniProt (https://www.uniprot.org/, [200]) were used to search terms "denervation", "response to denervation involved in regulation of muscle adaptation" (GO:0014894), "neuromuscular junction" (GO:0031594), "neuromuscular junction development" (GO:0007528), "skeletal muscle innervation", "axonogenesis involved in innervation" (GO:0060385), "skeletal muscle tissue regeneration" (GO:0043403), "axon regeneration" (GO:0031103), "aging", "cellular senescence" (GO:0090398), "replicative senescence" (GO:0090399), "positive regulation of cellular senescence" (GO:2000774), and "senescent cells". After the list was finalized, proteins were searched for in the detected proteins and if >90% of the samples included the given protein, the protein was included in our results. A total of 65 proteins are included herein.

Immunohistochemistry

Due to sample quality issues, n=20 older participants (55±8 years old, n=15 females, n=5 males) and n=11 younger participants (23±4 years old, n=6 females, n=5 males) were used for IHC. OCT-preserved samples were sectioned at a 7-µm thickness using a cryotome (Leica Biosystems; Buffalo Grove, IL, USA) and adhered to positively charged microscope slides.

Participants' trained and untrained VL muscle samples were placed on the same slides, as well as the PRE and POST sections to avoid batch-to-batch variation. Sections were then stored at -80°C until various staining procedures described in the paragraphs below.

For visualization of denervated myofibers, fiber type-specific fCSA and myonuclei number quantification, slides were air-dried for 90-120 minutes prior to a 10-minute acetone incubation at -20ºC. Slides were then incubated with 3% H_2O_2 for 10 minutes at room temperature followed by an incubation with autofluorescence quenching reagent for 1 min (TrueBlack; biotium, Fremont, CA, USA). Next, a block containing 5% goat serum, 2.5% horse serum, and 0.1% Triton-x was applied and incubated for one hour at room temperature. Another block was applied with streptavidin and then biotin solutions at room temperature for 15 minutes each. Following blocking, slides were incubated overnight at 4ºC with a primary antibody cocktail of 5.1H11 (NCAM) (mouse IgG1, 1:50, Developmental Studies Hybridoma Bank; Iowa City, IA, USA), BA-D5-c (Myosin Heavy Chain I) (mouse IgG2b, 1:100, Developmental Studies Hybridoma Bank), dystrophin (rabbit IgM, 1:100, GeneTex; Irvine, CA, USA; catalog #: GTX59790), and 2.5% horse serum in PBS. The next day, sections were incubated for 90 minutes in secondary biotin solution (anti-mouse IgG1, 1:1000, Jackson ImmunoResearch; West Grove, PA, USA), followed by a 60-minute incubation with a secondary cocktail containing AF647 anti-mouse IgG2b (1:200, Thermo Fisher Scientific; catalog #: A21242), AF555 anti-rabbit IgM (1:200, Thermo Fisher Scientific; catalog #: A21428), and Streptavidin, AF488 Conjugate (1:500, Thermo Fisher Scientific; catalog #: S32354). Lastly, slides were stained with 1:10,000 DAPI (4=,6-diamidino-2-phenylindole, Thermo Fisher Scientific; catalog #: D3571) for 10-minutes at room temperature before coverslips were applied with PBS and glycerol (1:1) as

mounting medium. Between each step, slides were washed in 1x phosphate buffered saline (PBS).

For quantification of satellite cell content and p21+ cells, a similar protocol was used. However, following the streptavidin and biotin block, the slides were incubated overnight at 4ºC with a primary antibody cocktail of Pax7 (mouse IgG1, 1:20, Developmental Studies Hybridoma Bank) and 2.5% horse serum in PBS. The following day, slides were incubated for 90 minutes in secondary biotin solution (anti-mouse IgG1, 1:1000, Jackson ImmunoResearch), followed by a 60-minute incubation with secondary streptavidin (1:500, SA-HRP, Thermo Fisher Scientific; catalog #: S-911), and a 20-minute incubation with TSA-555 (1:200, Thermo Fisher Scientific, catalog #: B-40957). Next, a block containing 5% goat serum, 2.5% horse serum, was applied, and incubated for 1 hour at room temperature. The next day sections were incubated for 90 minutes in secondary biotin solution (anti-rabbit IgG, 1:1000, Jackson ImmunoResearch), followed by a 60-minute incubation with a secondary cocktail containing AF647 anti-mouse IgG2b (1:200) and Streptavidin, AF488 Conjugate (1:500). Again, slides were stained with 1:10,000 DAPI for 10-minutes at room temperature before coverslips were applied with PBS and glycerol (1:1) as mounting medium.

The last IHC performed was for quantification of p16+ cells. This was an identical protocol to the satellite cell and p21 staining protocol except that the primary cocktail containing p21 was substituted for p16 (rabbit IgG, 1:200, Abcam, catalog #: ab51243).

Following mounting for all IHC procedures described above, slides were imaged using a fluorescent microscope (Nikon Instruments, Melville, NY) with the 20x objective lens. Fiber type fCSA, and myonuclear number were analyzed using open-sourced software MyoVision

[201]. Satellite cells, p21+ cells, and p16+ cells were manually quantified using Nikon NIS elements software (Nikon Instruments) and reported as cells per mm^2.

Statistical analysis

Statistical analyses were performed using SPSS (Version 26; IBM SPSS Statistics Software, Chicago, IL, United States). Prior to analysis, normality was assessed on all dependent variables using Shapiro–Wilk's tests. All comparisons between younger and older participants were analyzed using independent samples t-tests (for normally distributed data) or Mann-Whitney U-tests (for non-normally distributed data). Dependent samples t-tests were used for proteomic data to assess if training altered particular targets in older participants, and Wilcoxon signed-rank test were used for proteins that were non-normally distributed data. All other variables were analyzed using multi-factorial (within-within) two-way (leg*time) repeated measures ANOVAs. In the event a significant interaction was observed ($p<0.05$), the model was decomposed for within- and between-leg comparisons at PRE and POST. Pearson's correlations were also performed on select PRE (baseline) characteristics and change values on the change value of mCSA. Values between ±0.00-0.49 were considered weak, ±0.50-0.79 were noted as moderate, and values between ±0.80-0.99 were noted as strong [202]. Statistical significance was established at $p<0.05$. All data herein are presented in figures and tables as means ± standard deviation values, and figures (aside from proteomic data) also present individual respondent values.

CHAPTER IV

COMPLETED MANUSCRIPT

(to be submitted to Aging Cell following co-author edits and approval)

The effects of resistance training on denervated myofibers, senescent cells, and associated protein markers in middle-aged adults

Bradley A. Ruple[1], Madison L. Mattingly[1], Joshua S. Godwin[1], Mason C. McIntosh[1], Nicholas J. Kontos[1], Anthony Agyin-Birikorang[1], J. Max Michel[1], Daniel L. Plotkin[1], Shao-Yung Chen[2], Tim. N. Ziegenfuss[3], Andrew D. Fruge[4], L. Bruce Gladden[1], Austin T. Robinson[1], C. Brooks Mobley[1], Abigail L. Mackey[5,6], Michael D. Roberts[1,*]

Affiliations: [1]School of Kinesiology, Auburn University, Auburn, AL, USA; [2]Seer, Inc., Redwood City, CA, USA; [3]The Center for Applied Health Sciences, Canfield, OH, USA; [4]College of Nursing, Auburn University, Auburn, AL, USA; [5]Department of Clinical Medicine, Faculty of Health and Medical Sciences, University of Copenhagen, Copenhagen, DK; [6]Institute of Sports Medicine Copenhagen, Department of Orthopaedic Surgery, Copenhagen University Hospital – Bispebjerg and Frederiksberg, Copenhagen, Denmark

*Address correspondence to:
Michael D. Roberts, PhD
Professor, School of Kinesiology
Director, Nutrabolt Applied and Molecular Physiology Laboratory
Auburn University
301 Wire Road, Office 260
Auburn, AL 36849
Phone: 334-844-1925
Fax: 334-944-1467
E-mail: mdr0024@auburn.edu

ABSTRACT

While exercise is beneficial for aging skeletal muscle, the mechanisms are incompletely understood. Thus, we sought to examine how eight weeks of unilateral leg extensor resistance training (2d/week) affected denervated myofibers, senescent stromal cells, and associated protein markers in untrained, middle-aged participants (MA, 55±8 years old, 17 females, 9 males). Vastus lateralis (VL) ultrasound images, biopsies, and strength assessments were obtained from the trained and untrained legs prior to (PRE) and following the intervention (POST). Type I/II/mixed fiber cross-sectional areas (fCSA), satellite cells (Pax7+), denervated myofibers (NCAM+), and senescent cells (p16+ or p21+) were assessed in 20 of these participants. In the trained leg of a subset of these participants, proteomics data was manually interrogated to examine proteins associated with muscle-nerve communication and senescence (n=18), and a targeted antibody-based array was used to examine senescence-associated secretory phenotype (SASP) protein expression (n=13). Leg extensor peak torque increased with training ($p<0.001$), and an interaction for muscle cross-sectional area approached significance ($p=0.082$) whereby hypertrophy favored the trained leg. While no significant interactions existed for I/II/mixed fCSAs, the percentage of NCAM+ type I/II/mixed myofibers, or senescent (p16+ or p21+) cells, a significant interaction ($p=0.037$) was evident for satellite cells whereby an increase occurred in the trained leg ($p=0.020$). Interestingly, while >90% satellite cells were not p16+ or p21+, most p16+ and p21+ cells were also Pax7+ (>90% on average) indicating that most senescent cells were satellite cells. Training altered 13/46 detected proteins related to muscle-nerve communication (all upregulated, $p<0.05$) and 10/19 proteins related to cellular senescence (9 upregulated, $p<0.05$). Of the SASP proteins, only 1/17 markers increased with training (IGFBP-3, $p=0.031$). In conclusion, while several proteins associated with muscle-nerve communication

were upregulated in MA participants with training, NCAM+ myofibers were not altered. Moreover, resistance training in MA participants increased the abundance of senescence-related proteins in skeletal muscle, albeit this did not coincide with alterations in senescent cell numbers or SASP proteins. Finally, given that p16+ or p21+ were not affected with training, we speculate that the training-induced increase in satellite cells or the proliferation of an unidentified cell type may have accounted for the increases in senescence-related proteins, and that resistance training is not a driver of cellular senescence.

Keywords: aging, muscle, resistance training, denervation, senescence

INTRODUCTION

Skeletal muscle is a tissue that is responsible for force generation, locomotion, metabolism, and heat production [1]. Skeletal muscle consists of thousands of muscle fibers, or myofibers, and each fiber is innervated by a single alpha motor neuron branch. This neuron, and all the myofibers it innervates, is collectively termed a motor unit. Functionally, the motor unit is responsible for relaying signals from the nervous system to the muscle to elicit muscle contraction. However, the site of muscle-nerve communication can be altered, specifically the neuromuscular junction (NMJ) [2, 3]. When a motor neuron is no longer communicating with a myofiber, this is referred to as denervation [5]. With aging there is an acceleration of denervation and a concomitant decline in reinnervation [6, 7]. Additionally, a preferential denervation of type II fibers occurs whereby the denervated myofibers are re-innervated by lower-threshold motor units, a phenomenon termed fiber type grouping [3]. Another well-established characteristic of aging is sarcopenia, or age-related muscle loss [8], and losses in myofiber innervation could partially explain why age-related atrophy ensues. In this regard, neural cell adhesion molecule-positive (NCAM+) myofibers (indicative of denervation) are higher in older versus younger individuals, thus providing evidence that this phenomenon occurs [9, 10]. While there have been multiple studies showing the benefits of exercise for older individuals [11-15], there is limited and equivocal research on how exercise training affects denervated myofibers [16-19]. Furthermore, older individuals exhibit blunted hypertrophic responses to resistance training, and a recent meta-analysis supports that increased myofiber hypertrophy to resistance training is inversely related with age [20]. These data could be explained, in part, by the presence of more denervated myofibers and/or altered NMJ characteristics in aged individuals.

A diminished hypertrophic response to resistance training in older individuals may also be, in part, due to an increased presence of senescent cells. p16 (cyclin dependent kinase inhibitor 2A; $p16^{INK4a}$) and p21 (cyclin dependent kinase inhibitor 1A; $p21^{WAF1/CIP1}$) are markers of senescence that inhibit cyclin-dependent kinases and promote cell cycle arrest [21-23]. Senescent cells are defined as a cell type in the interstitium that enters a state of semi-permanent cell cycle arrest and loses its regenerative capacity, while secreting molecules associated with inflammation (i.e., senescence-associated secretory phenotype, or SASP) [24]. Aging is positively associated with senescent cell abundance in muscle tissue [203-205]. Specifically, older mice present more senescent cells in the extracellular matrix of the plantaris muscle in response to synergist ablation-induced mechanical overload (but not in the basal state) relative to younger adult mice and this coincides with an impairment in muscle hypertrophy [25]. However, a senolytic cocktail (i.e., dasatinib and quercetin, or D+Q) reduced the presence of senescent cells in older mice and rescued the impaired hypertrophic phenotype. While these data are informative, little is known regarding the association between senescent cell abundance and the hypertrophic response to resistance training in older humans.

Given the knowledge gaps in humans discussed above, the purpose of this study was multifaceted. First, we sought to examine how eight weeks of unilateral knee extensor resistance training affected the number of denervated (NCAM+) myofibers and senescent cells (p16+ or p21+) in middle-aged individuals (MA) in both the trained and non-trained legs. Additionally, we implemented deep proteomics and targeted antibody array approaches to examine how proteins associated with cellular senescence and muscle-nerve communication were affected in the trained leg of these individuals. As with some of our past research [160, 206], we also sought to examine if resistance training elicited rejuvenating effects on assayed targets. Thus, tissue

from a college-aged cohort (denoted as "Y" throughout) was used to examine if any aging or "training-rejuvenating" effects existed for the outcome variables. We hypothesized that, prior to training, both legs of the MA participants would possess more denervated myofibers and senescent cells compared to Y participants. We also hypothesized that resistance training would decrease the number of denervated myofibers and associated proteins in the training leg. Finally, given that senescent cells increase with age and stress, we hypothesized that senescent cells and proteins associated with cellular senescence would increase in the trained leg of MA participants.

METHODS

Ethical approval and participant screening

This study was a non-related sub-aim of a study approved by the Auburn University Institutional Review Board (IRB protocol #21-461 MR 2110) which aimed to investigate the effects of a nutritional supplement (312 mg of combined Wasabia japonica extract, theacrine, and copper (I) niacin chelate) versus a placebo on unrelated markers over an eight-week period. A unilateral leg resistance training (2d/week) protocol was implemented to perform non-supplementation secondary analyses as presented herein. To ensure supplementation did not have appreciable effects on the assayed targets, we statistically compared the placebo and supplementation groups for pre-to-post intervention change scores in phenotypes (n=13 per group) histology (n=10 per group), targeted proteomics (n=9 per group), and SASP protein markers (n=6-7 per group). No significant differences in these scores were observed between supplementation groups for the following variables in the training leg or non-training leg: vastus lateralis (VL) muscle cross-sectional area (mCSA) ($p=0.693$ and $p=0.919$, respectively), mixed

fiber cross-sectional area (fCSA) ($p=0.187$ and $p=0.333$, respectively), the percentage of NCAM+ myofibers ($p=0.803$ and $p=0.768$, respectively), satellite cell number ($p=0.131$ and $p=0.705$, respectively), or p21+/Pax7+ cell counts ($p=0.360$ and $p=0.322$, respectively), or p16+/Pax7+ cell counts ($p=0.376$ and $p=0.900$, respectively). Of the 66 targeted proteins from the proteomic analysis (only performed in the trained leg), only one was affected with supplementation (MTR, related to "axon regeneration", was downregulated, $p=0.043$). Of the 17 targeted SASP proteins (only performed in the trained leg), five showed significant change score differences between supplementation groups exceeding $p<0.05$ according to the Mann-Whitney U statistic (GM-CSF, IGFBP3, IL-6, IL-8, and RANTES). Wilcoxon rank tests indicated that the increase in IGFBP3 was the only significant SASP marker to increase in the 6 participants that consumed the nutritional supplement ($p=0.031$). Conversely, Wilcoxon rank tests indicated that IL-6 ($p=0.047$) and IL-8 ($p=0.016$) significantly decreased in the 7 participants that consumed the placebo supplement. Hence, given the marginal differences between supplementation groups for training outcomes, histology markers, proteomic targets, and SASP proteins, we opted to combine the two groups to robustly increase our statistical power for this secondary analysis.

Tissue from two prior studies were also used (Protocol #19–249 MR 1907 and #20–136 MR 2004) whereby strength, VL ultrasound images, and VL biopsies were obtained from younger adults [192, 193]. While the younger participants were involved in training studies, the participants' basal (pre-intervention) characteristics were used to examine whether training leg outcomes in MA participants were altered to "youth-like" levels. Due to tissue or resource limitations, subsets of MA and Y participants were analyzed for certain assays, and these details are provided in Table 1.

Table 1. Participant n-sizes for outcome variables

Outcome	MA participants	Y participants
General phenotypes	26 (age: 55±8 years old; 9M/17F)	15 (age: 22±3 years old; 6M/9F)
Histology variables	20 (age: 55±8 years old; 5M/15F)	11 (age: 22±3 years old; 5M/6F)
Targeted proteomics*	18 (age: 55±8 years old; 4M/14F)	9 (age: 22±2 years old; 2M/7F)
SASP proteomics*	13 (age: 58±8 years old; 3M/10F)	5 (age: 22±1 years old; 1M/4F)

Notes: *, indicates that assays were only performed in the trained leg of MA participants.

Inclusion criteria for all studies indicated that participants had to possess a body mass index <34 kg/m^2, have no or minimal experience with resistance training (≤ 1 day/week) one year prior to the study, and be free of any medical condition that would contraindicate participating in an exercise program or donating skeletal muscle biopsies. Participants provided verbal and written consent to participate prior to data collection and the study conformed to standards set by the latest revision of the Declaration of Helsinki except for being registered as a clinical trial.

Study Design and Training Paradigm

The resistance training intervention consisted of supervised unilateral leg extensions (2d/week for 8 weeks), and the intervention was preceded and followed by strength and VL muscle assessments (described later). For logistical purposes, all MA participants trained their right legs, with the left leg serving as a within-participant, untrained control leg. From testing, 13 of the 26 right legs were considered the dominant leg as measured by 3-repetition max (3RM) testing (described below).

For each training day, participants performed five sets of 12 repetitions per session. The beginning training load was established at ~40% of the participant's 3RM (described below). After each set, participants verbally articulated their perceived repetitions in reserve (RIR), and training load was adjusted accordingly. RIR values of 0-2 after a set resulted in no training load change in each session. RIR values of 3-5 for consecutive sets resulted in the training load being increased by 5-10%. For RIR values ≥6 after one set, the training load was increased by 10-20%.

If the weight could not be performed with full range of motion, or the participant could not complete 12 repetitions for a given set, the training load was decreased.

Strength testing

The first and last workout of the eight-week training paradigm consisted of maximal leg extensor-flexion torque assessments using isokinetic dynamometry (Biodex System 4; Biodex Medical Systems, Inc., Shirley, NY, USA) and 3RM leg extensor strength testing. Notably, both legs were used for these assessments. Prior to dynamometer testing, the participant's lateral epicondyle was aligned with the axis of the dynamometer's lever arm, and the hip was positioned at 90°. The starting leg was randomized for everyone prior to each test. The participant's shoulders, hips, and leg were strapped and secured for isolation during testing. Following three warm-up trials at a submaximal effort, participants completed five maximal voluntary isokinetic knee extension and flexion actions at 60 degrees/second. Participants were provided verbal encouragement during each contraction. The isokinetic contraction resulting in the greatest peak torque value was used for analyses. Participants were given a one-minute rest and then the contralateral leg completed this exact protocol. Approximately five minutes following isokinetic dynamometry testing, participants performed 3RM strength testing on both the right and left leg. Prior to testing, participants were given a warm-up load and instructed to complete 10 repetitions. After participants recorded their RIR for the warmup set, the weight was adjusted accordingly for another warm-up set of five repetitions. RIR was recorded again to determine the participant's starting load for a 3RM attempt. The load was incrementally increased 5-10% per 3RM attempt until 3RM testing concluded, indicated by failure of full range of motion on any of the repetitions, or if RIR recorded was 0. Participants were allowed a full three minutes of

recovery between attempts. The isokinetic dynamometry and 3RM testing described herein was similar for both the first and final workout.

Testing Sessions

Urine specific gravity testing for hydration. Participants performed a testing battery prior to the start of training (PRE) and 3-5 days following the last resistance training workout (POST). Participants arrived for testing at a minimum of 4 hours fasted and well hydrated. Upon arrival participants submitted a urine sample (~5 mL) for urine specific gravity assessment (USG). Measurements were performed using a handheld refractometer (ATAGO; Bellevue, WA, USA). USG levels in all participants were ≤ 1.020, indicating sufficient hydration [194].

Body composition testing. Once adequate hydration was determined, body composition was assessed using multi-frequency bioelectrical impedance analysis (InBody 520, Biospace, Inc. Seoul, Korea). From the scan, body fat percentage was recorded. Previously determined test-retest reliability yielded an intraclass correlation coefficient ($ICC_{3,1}$) of 0.99, standard error of the measurement (SEM) of 0.87%, and minimal difference (MD) of 1.71% for body fat percentage.

Ultrasonography assessment for muscle morphology. A detailed description of VL assessments using ultrasonography has been published previously by Ruple et al. [195]. Briefly, real-time B-mode ultrasonography (NextGen LOGIQe R8, GE Healthcare; Chicago, IL, USA) using a multifrequency linear-array transducer (L4-12T, 4–12 MHz, GE Healthcare) was used to capture right and left leg images to determine VL muscle cross-sectional area (mCSA). Prior to scans, the mid-thigh of the leg was determined by measuring the total distance from the mid-inguinal crease in a straight line to the proximal patella, with the knee and hip flexed at 90°, a mark was made using a permanent marker at 50% of the total length. From that location, a permanent marker was used transversely to mark the mid-belly of the VL. This marking is where

all PRE ultrasound images were taken as well as the muscle biopsy (described below). POST images were taken at the PRE biopsy scar to ensure location consistency between scans. During mCSA scans, a flexible, semirigid pad was placed around the thigh and secured with an adjustable strap to allow the probe to move in the transverse plane. Using the panoramic function of the device (LogicView, GE Healthcare), images were captured starting at the lateral aspect of the VL and moving medially until rectus femoris was visualized, crossing the marked location. All ultrasound settings were held constant across participants and laboratory visits (frequency: 10 MHz, gain: 50 dB, dynamic range: 75), and scan depth was noted and held constant across time points per participant. Images were downloaded and analyzed offline using ImageJ software (National Institutes of Health, Bethesda, MD). All ultrasound images were captured and analyzed by the same investigators at each timepoint. Previously determined test-retest reliability on 10 participants measured twice within 24 h (where BAR captured images and JSG analyzed images) yielded an ICC of 0.99, SEM of 0.60 cm^2, and MD of 1.65 cm^2 for VL mCSA.

Collection of muscle tissue. Muscle biopsies were obtained at PRE and POST, from the mid-belly of both the right and left VL muscle, with sampling time of day at PRE and POST being standardized for each participant. Lidocaine (1%, 1.0 mL) was injected subcutaneously superficial to the skeletal muscle fascia at the previously marked location. After five minutes of allowing the anesthetic to take effect, a small pilot incision was made using a sterile Surgical Blade No. 11 (AD Surgical; Sunnyvale, CA), and the 5-gauge biopsy needle was inserted into the pilot incision ~1 cm below the fascia. Approximately 50–80 mg of skeletal muscle was removed using a double chop method with applied suction. Following biopsies, tissue was rapidly teased of blood and connective tissue. A portion of the tissue (~10–20 mg) was preserved in freezing media for histology (OCT; Tissue-Tek, Sakura Finetek Inc; Torrence, CA,

USA), slowly frozen in liquid nitrogen-cooled isopentane, and subsequently stored at −80°C until histological analysis. Another portion of the tissue (~30–50 mg) was placed in pre-labeled foils, flash frozen in liquid nitrogen, and subsequently stored at −80°C until other assays described below.

Deep Proteomics for the Manual Interrogation of Denervation and Senescence-related Proteins

Sample Preparation. Sarcoplasmic protein isolation for all samples occurred at Auburn University using a previously described method [196], and the complete methods used have been previously described with a subset of the current participants [207]. Approximately 30 mg of tissue was homogenized using tight-fitting pestles in 500 µL of 25 mM Tris, pH 7.2, 0.5% Triton X-100 (with added protease inhibitors; Promega, Cat. No. G6521; Madison, WI, USA). Samples were then centrifuged at 1500 g for 10 min at 4°C and the soluble/sarcoplasmic fraction supernatants were collected. Due to resource constraints, 18 MA participants' PRE and POST trained leg specimens and 9 younger participant specimens were used for further analysis.

Proteomics analysis of the sarcoplasmic fraction was performed at Seer, Inc. (Redwood City, CA, USA). For each sample, 250 µL soluble/sarcoplasmic fraction supernatant was subjected to the Seer Proteograph Assay protocol [197]. After the samples were loaded onto the SP100 Automation Instrument, they were subjected to protein corona formation and processing to generate desalted purified peptides protein identification using Reversed Phase (RP) Liquid Chromatography coupled to Mass spectrometry (LC-MS). To form the protein corona, Seer's proprietary nanoparticles (NPs) were mixed with the samples and incubated at 37°C for 1 hr. Unbound proteins were removed prior to downstream wash, reduction, alkylation, and protein digestion steps which were performed according to Seer's Proteograph Assay protocol [197].

LC-MS configuration. Peptides obtained from each of the five NP mixtures were separately reconstituted in a solution of 0.1% formic acid and 3% acetonitrile [198] spiked with 5 fmol µL PepCalMix from SCIEX (Framingham, MA, USA). Reconstitution volumes varied NPs to allow for constant peptide quantity for MS injection between samples regardless of starting volume (240 ng: NP1, 400 ng: NP2, 360 ng: NP3, 120 ng: NP4, and 320 ng: NP5). 4 µL of each sample were analyzed with a Ultimate3000 RLSCnano LC system coupled with a Orbitrap Fusion Lumos mass spectrometer (Thermo Fisher; Waltham, MA, USA). Peptides were loaded on an Acclaim PepMap 100 C18 (0.3 mm ID × 5 mm) trap column and then separated on a 50 cm µPAC analytical column (PharmaFluidics, Belgium) at a flow rate of 1 µL/min using a gradient of 5–25% solvent B (100% ACN) mixed into solvent A (100% water) over 26 min. The mass spectrometer was operated in Data Independent Acquisition mode using 10 m/z isolation windows from 380-1200 m/z and 3 s cycle time. MS1 scans were acquired at 60k resolution and MS2 at 30k resolution.

Data Processing. Data-independent acquisition LC-MS data were processed using Proteograph Analysis Suite (PAS) v2.1 (Seer, Inc) using the DIA-NN search engine (version 1.8.1) in library-free mode searching MS/MS spectra against an in silico predicted library based on Uniprot's Homo Sapiens reference database (UP000005640_9606, download December 9th, 2022). Library free search parameters included trypsin, 1 missed cleavage, N-terminal Met excision, fixed modification of Cys carbamidomethylation, peptide length of 7-30 amino acids, precursor range of 300-1800 m/z, and fragment ion range of 200-1800 m/z. Heuristic protein inference was enabled, MS1 and MS2 mass accuracy was set to 10 ppm. Precursor FDR was set to 0.01, and PG q-value was set to 0.01. Quantification was performed on summed abundances of all unique peptides considering only precursors passing the q-value cutoff. PAS summarizes

all nanoparticle values for a single protein into a single quantitative value. Specifically, a single protein may have been measured up to five times, once for each nanoparticle. To derive the single measurement value, PAS uses a maximum representation approach, whereby the single quantification value for a particular peptide or protein group represents the quantitation value of the NP which most frequently has measured any given proteins across all samples. The relative abundances of protein targets were obtained by normalizing raw spectral values for each identified protein to total spectra within-participant. After normalization, for proteins that were not detected, values were set at zero with the assumption the protein was in low abundance or not detected.

An *a priori* systematic search was performed to filter the number of proteins used for the current analysis. Specifically, Gene Ontology (GO; http://geneontology.org, [199]) and UniProt (https://www.uniprot.org/, [200]) were used to search terms “denervation”, “response to denervation involved in regulation of muscle adaptation” (GO:0014894), “neuromuscular junction” (GO:0031594), “neuromuscular junction development” (GO:0007528), “skeletal muscle innervation”, “axonogenesis involved in innervation” (GO:0060385), “skeletal muscle tissue regeneration” (GO:0043403), “axon regeneration” (GO:0031103), “aging”, “cellular senescence” (GO:0090398), “replicative senescence” (GO:0090399), “positive regulation of cellular senescence” (GO:2000774), or “senescent cells”. After the list was finalized, proteins belonging to these GO terms were manually interrogated. This approach yielded 65 proteins, with 46 being related to muscle-nerve communication and 19 being related to cellular senescence.

SASP protein detection in muscle tissue

Sarcoplasmic protein isolates (80 µg protein) from the trained leg of a subset of MA participants (n=13) and younger participants (n=5) were subjected to a customized antibody-based fluorometric array containing SASP proteins (RayBiotech; Peachtree Corners, GA, USA; Cat. No.: AAH-CYT-G5-4). Samples were diluted 80 µg of total protein in 120 µl of blocking buffer and added into the array to incubate for two hours. After washing, the arrays were incubated first, with a biotin-conjugated anti-cytokine antibody mix and then a 555 streptavidin-fluorophore, both for two hours. All incubations were performed at room temperature with gentle rotation and washes before the next step. The array was then read using an MDC GenePix 4200A Microarray Scanner (Molecular Devices; San Jose, CA, USA). Expression readings for each SASP marker were calculated as follows (Equation 1):

Equation 1:

$$\text{SASP protein expression} = \frac{\text{protein duplicate median} - \text{neg. control replicate median}}{\text{positive control replicate median}}$$

Zeros were substituted for proteins that yielded negative values (i.e., the signal was less than the negative control). All data are presented as relative expression units.

Immunohistochemistry

Due to sample quality issues, n=20 MA participants (55±8 years old, n=15 females, n=5 males) and n=11 Y participants (23±4 years old, n=6 females, n=5 males) were used for immunohistochemistry. OCT-preserved samples were sectioned at 7 µm thickness using a cryotome (Leica Biosystems; Buffalo Grove, IL, USA) and adhered to positively charged slides. Participants' trained and untrained leg muscle samples were placed on the same slides, as well as the PRE and POST sections to avoid batch-to-batch variation. Sections were then stored at -80°C until various staining procedures described in the following paragraphs.

The following methods were employed for the detection of denervated myofibers, fiber type-specific cross-sectional areas (fCSA) and myonuclei quantification. Slides were air-dried for 90-120 minutes prior to a 10-min acetone incubation at -20ºC. Slides were then incubated with 3% H_2O_2 for 10 minutes at room temperature followed by an incubation with autofluorescence quenching reagent for 1 min (TrueBlack; biotium, Fremont, CA, USA). Next, a block containing 5% goat serum, 2.5% horse serum, and 0.1% Triton-X was applied and incubated for 1 h at room temperature. Another block was applied with streptavidin and then biotin solutions (Streptavidin/Biotin Blocking Kit, Vector Labs; Newark, CA, USA; Cat. No.: SP2002) at room temperature for 15 min each. Following blocking, slides were incubated overnight at 4ºC with a primary antibody cocktail of NCAM (mouse IgG1, 1:50, Developmental Studies Hybridoma Bank; Iowa City, IA, USA; Cat. No. 5.1H11), myosin heavy chain I (mouse IgG2b, 1:100, Developmental Studies Hybridoma Bank; Cat. No. BA-D5-c), dystrophin (rabbit IgM, 1:100, GeneTex; Irvine, CA, USA; Cat. No.: GTX59790), and 2.5% horse serum in PBS. The next day, sections were incubated for 90 min in secondary biotin solution (anti-mouse IgG1, 1:1000, Jackson ImmunoResearch; West Grove, PA, USA), followed by a 60-min incubation with a secondary cocktail containing AF647 anti-mouse IgG2b (1:200, Thermo Fisher Scientific; Cat. No.: A21242), AF555 anti-rabbit IgM (1:200, Thermo Fisher Scientific; Cat. No.: A21428), and Streptavidin, AF488 Conjugate (1:500, Thermo Fisher Scientific; Cat. No.: S32354). Lastly, slides were stained with 1:10,000 DAPI (4’,6-diamidino-2-phenylindole, Thermo Fisher Scientific; Cat. No.: D3571) for 10 min at room temperature before coverslips were applied with PBS and glycerol (1:1) as mounting medium. Between each step, slides were washed in 1x phosphate buffered saline (PBS).

For quantification of satellite cells (Pax7+) and p21+ cells, a similar protocol was used. However, following the streptavidin and biotin block, the slides were incubated overnight at 4ºC with a primary antibody cocktail of Pax7 (mouse IgG1, 1:20, Developmental Studies Hybridoma Bank) and 2.5% horse serum in PBS. The following day, slides were incubated for 90 min in secondary biotin solution (anti-mouse IgG1, 1:1000, Jackson ImmunoResearch), followed by a 60-min incubation with secondary streptavidin (1:500, SA-HRP, Thermo Fisher Scientific; Cat. No.: S-911), and a 20-min incubation with TSA-555 (1:200, Thermo Fisher Scientific, Cat. No.: B-40957). Next, a block containing 5% goat serum, 2.5% horse serum, was applied, and incubated for 1 h at room temperature. Similar steps from the fCSA/myonuclei/NCAM stain were applied except that the primary antibody cocktail included p21 (rabbit IgG, 1:200, Abcam; Cambridge, MA, USA; Cat. No. ab109199), dystrophin (mouse IgG2b, 1:100, Developmental Studies Hybridoma Bank; Cat. No. Mandys8 (8H11), and 2.5% horse serum in PBS. The next day sections were incubated for 90 min in secondary biotin solution (anti-rabbit IgG, 1:1000, Jackson ImmunoResearch) followed by a 60-min incubation with a secondary cocktail containing AF647 anti-mouse IgG2b (1:200) and Streptavidin, AF488 Conjugate (1:500). Again, slides were stained with 1:10,000 DAPI for 10 min at room temperature before coverslips were applied with PBS and glycerol (1:1) as mounting medium.

The last IHC performed was for quantification of p16+cells. The staining protocol was identical to the satellite cell and p21 staining protocol except that the primary cocktail containing p21 (rabbit IgG, 1:200, Abcam; Cambridge, MA, USA, ab109199), was substituted for p16 (rabbit IgG, 1:200, Abcam; Cambridge, MA, USA, ab51243).

Immediately following the mounting procedure for each stain, slides were imaged using a fluorescent microscope (Nikon Instruments, Melville, NY, USA) with the 20x objective lens.

Four to six fields of view were captured per participant time point. fCSA and myonuclear number were analyzed using open-sourced software MyoVision [201]. Satellite cells, p21+ cells, and p16+ cells were manually quantified using Nikon NIS elements software (Nikon Instruments) and reported as number per 100 fibers.

Statistical analysis

Statistical analyses were performed using SPSS (Version 26; IBM SPSS Statistics Software, Chicago, IL, United States). Prior to analysis, normality was assessed on all dependent variables using the Shapiro–Wilk's test. All comparisons between MA and Y participants were analyzed using independent samples t-tests (for normally distributed data) or Mann-Whitney U-tests (for non-normally distributed data). Dependent samples t-tests were used for proteomic and SASP protein data to assess if training altered targets in MA participants, and Wilcoxon signed-rank tests were used for non-normally distributed data. All other variables were analyzed using multi-factorial (within-within) two-way (leg*time) repeated measures ANOVAs (or Freidman's tests for non-normally distributed data), and in the event a significant interaction was observed ($p<0.05$), the model was decomposed for within- and between-leg comparisons at PRE and POST using parametric or non-parametric post hoc tests. Statistical significance was established at $p<0.05$. Eta square (η^2) effect sizes are also provided for certain between-group comparisons and interactions, and effect size ranges were classified as follows: <0.06 = small effect, 0.06–0.14 moderate effect, and >0.14 large effect. All data herein are presented in figures and tables as means ± standard deviation values, and figures (aside from proteomic and SASP data) also present individual respondent values.

RESULTS

Participant characteristics

Baseline participant characteristics can be found in Table 2. Briefly, 26 participants (55±8 years old, n=17 females, n=9 males) completed the eight weeks of unilateral knee extensor resistance training, and general phenotype and training outcomes were collected for all these participants. However, as previously stated, only 20 MA participants yielded muscle samples suitable for histology (55±8 years old, n=15 females, n=5 males), and deep proteomics was performed for only 18 MA participants' PRE- and POST-intervention trained leg due to resource constraints (55±8 years old, n=14 females, n=4 males). A subset of the fifteen Y participants (22±4 years old, n=9 females, n=6 males) were included for age comparison purposes. While estradiol levels in the Y females was numerically greater than the MA females, this was non-significant (502 ± 95 pg/mL versus 539 ± 119 pg/mL, p=0.465). This trend held with the removal of the four MA females on menopausal treatment prescriptions (p=0.155). Eleven of these 15 Y participants (23±4 years old, n=6 females, n=5 males) yielded tissue adequate for IHC comparisons to the 20 MA participants, and muscle tissue from 9 of these 15 Y participants (22±2 years old, n=7 females, n=2 males) were used for proteomic comparisons to the MA participants. Besides age (p<0.001), there were no significant differences in general anthropometrics between the 26 MA and 15 Y participants.

Table 2. Participant characteristics

Variable	MA (n=26)	Y (n=15)	p-value
Age (years)	55±8	23±4	<0.001
Height (cm)	168.3±10.4	171.9±5.9	0.223
Body Mass (kg)	73.5±14.8	73.7±11.1	0.966
Percent Body Fat (%)	28.9±8.6	30.38±9.5	0.609
Fat Mass (kg)	21.4±7.9	22.9±9.1	0.574
Fat Free Mass (kg)	52.2±12.1	48.7±7.4	0.323
Body Mass Index (kg/m^2)	25.8±3.8	25.0±3.4	0.464
Fiber Type I (%)*	46.9±15.3	40.7±13.9	0.361

Fiber Type II (%)*	53.1±15.3	59.3±13.9	0.259

Legend: Data are presented as means ± standard deviation values. Abbreviation: MA, middle-aged participants; Y, younger participants. *, indicates data is from 20 MA participants and 11 Y participants.

General Training Adaptations

Figure 1 depicts PRE and POST data in MA participants and basal state data in Y participants for VL mCSA, leg extension peak torque, and VL fCSA. While there was a significant leg (L) ($p=0.047$, $\eta^2=0.174$) and time (T) effect ($p=0.048$, $\eta^2=0.067$), there was not a significant leg x time (LxT) interaction for VL mCSA (trained leg: 20.19±5.20 cm^2 to 20.64±5.03 cm^2, untrained leg: 19.62±5.03cm^2 to 19.62±5.05cm^2, $p=0.082$, $\eta^2=0.116$, Fig. 1a). Additionally, there were no significant differences in values between MA and Y participants at any time point. A Friedman test was conducted to assess differences in leg extension peak torque across the groups. The test yielded a significant result ($p=0.005$), and Wilcoxon tests indicated significantly greater values in the trained leg after training ($p<0.001$) as well as the trained versus untrained leg at the post-intervention time point ($p=0.011$). However, there was no significant difference between MA and Y participants at any time point. Next, there were no significant effects of L, T, or LxT in type I (L: $p=0.101$; T: $p=0.328$; LxT: $p=0.906$, Fig. 1e), type II (L: $p=0.923$; T: $p=0.195$; LxT: $p=0.437$, Fig. 1f), or mixed fCSA (L: $p=0.403$; T: $p=0.344$; LxT: $p=0.549$, Fig. 1g). While type I fCSA yielded no significant differences between MA and Y participants at any time point, type II fCSA was significantly lower at all times in MA versus Y participants ($p=0.005$-0.017), and mixed fCSA was significantly lower only in the POST trained leg ($p=0.035$). Lastly, there were no significant effects of L, T, or LxT for average myonuclei for type I fibers (L: $p=0.461$; T: $p=344$; LxT: $p=0.563$) or type II fibers (L: $p=0.451$; T: $p=0.420$; LxT: $p=0.209$) (*data not graphed*). In addition, MA compared to Y participants had significantly

more myonuclei per type I fibers in both legs at PRE (p=0.035 for both) but not at POST, or in type II fibers at PRE or POST (*data not graphed*).

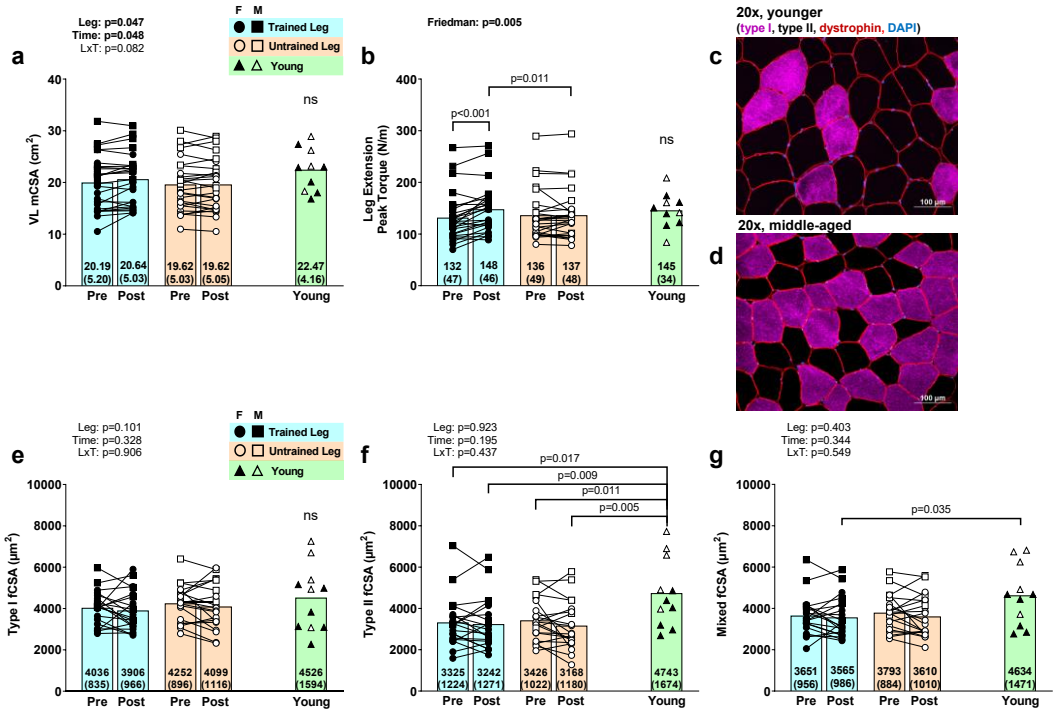

Figure 1. General training adaptations

Legend: Variables presented include vastus lateralis muscle cross-sectional area (a), leg extensor peak torque at 60°/sec in newton-meters (b), type I fiber cross-sectional area (e), type II fiber cross-sectional area (f), and mixed fiber cross-sectional area (g). Panels (a) and (b) contain n=26 middle-aged (MA) participants (55±8 years old, n=17 females, n=9 males) and n=10 Y participants (23±4 years old, n=6 females, n=4 males). Panels (e-g) contain n=20 MA participants (55±8 years old, n=15 females, n=5 males) and n=11 Y participants (23±4 years old, n=6 females, n=5 males). Representative images for fiber cross-sectional area for Y and MA participants are presented in panels c and d. Data are presented as mean ± standard deviation values for PRE and POST intervention MA-trained and MA-untrained leg, and the Y comparator group. Individual responses are also illustrated, with open circles and squares indicating females and males, respectively, for the MA-untrained leg and closed circles and squares indicating females and males, respectively, for the MA-trained leg. Open and closed triangles indicate Y females and males, respectively.

Denervated myofibers

For NCAM+ fiber quantification, a total of 184±78 and 162±67 fibers were counted prior to the eight weeks and 187±88 and 183±67 fibers after eight weeks for the trained and untrained legs, respectively. A Friedman test indicated that the percent of NCAM+ fibers in MA participants was not significantly different between legs for mixed (p=0.180, Fig. 2a), type I (p=0.061, Fig. 2b), or type II fibers (p=0.865, Fig. 2c). Interestingly, for both mixed NCAM+ fibers and NCAM+ type I fibers, the percentage of PRE trained (p≤0.006) and POST untrained leg (p≤0.010) were significantly higher than the Y cohort according to Mann-Whitney U tests. In contrast, only the POST trained leg was significantly higher than the Y cohort for percentage of type II NCAM+ fibers (p=0.022) according to a Mann-Whitney U test.

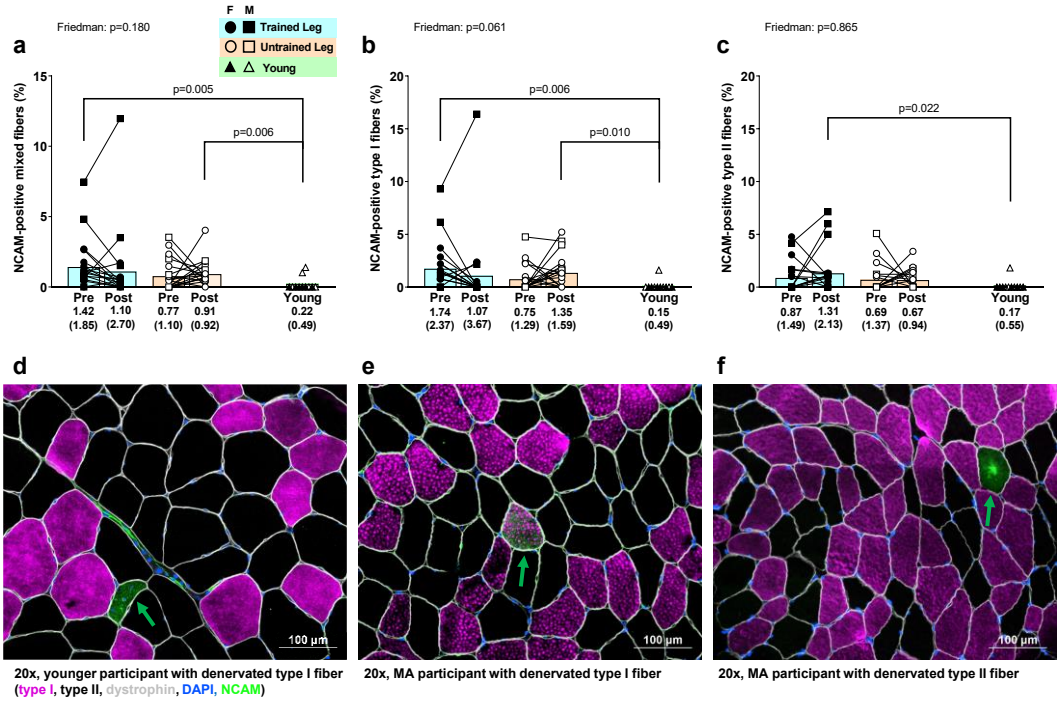

Figure 2. Immunohistochemistry for denervated myofibers
Legend: Variables presented include percent of mixed fibers that were NCAM+ (a), percent of type I fibers that were NCAM+ (b), percent of type II fibers that were NCAM+ (c). Panels a-c contain n=20 middle-aged (MA) participants (55±8 years old, n=15 females, n=5 males) and n=11 Y participants (23±4 years old, n=6 females, n=5 males). Representative 20x images are presented in panels d-f whereby green arrows depict NCAM+ myofibers. Data are presented as mean ± standard deviation values for PRE and POST MA-trained and MA-untrained leg, and the

Y comparator group. Individual responses are also illustrated, with open circles and squares indicating females and males, respectively, for the MA-untrained leg and closed circles and squares indicating females and males, respectively, for the MA-trained leg. Open and closed triangles indicate Y females and males, respectively.

Satellite Cells and Senescent Cells

A significant LxT interaction was evident for satellite cells (trained leg: 7.9±3.4 to 10.4±6.0 cells/100 fibers; untrained leg: 8.5±4.2 to 8.2±1.8 cells/100 fibers, $p=0.037$, $\eta^2=0.209$, Fig. 3a). While PRE to POST values significantly increased in the training leg ($p=0.020$), POST values between legs were not significantly different ($p=0.091$). Additionally, satellite cell number for both MA participant legs at PRE and the untrained leg at POST were significantly lower ($p\leq0.018$) than the Y cohort, but the values in the POST training leg were not ($p=0.073$). For p21+ cell quantification, a total of 206±79 and 189±69 fibers were counted prior to the eight weeks and 201±70 and 210±82 fibers after eight weeks for the trained and untrained legs, respectively. The Friedman test indicated the total number of p21+ cells in MA participants (both Pax7+ and Pax7-) was not significant between legs ($p=0.138$, Fig. 3b). However, compared to the Y cohort, Mann-Whitney U tests indicated that there was a significantly greater number of these cells in both legs, at both timepoints ($p\leq0.021$). For p21+ satellite cells (p21+/Pax7+) in MA participants, a Friedman test revealed there was no significant effect between legs ($p=0.162$, Fig. 3e). Again, compared to the Y cohort, there was a significantly greater amount of these cells in both legs, at both timepoints ($p\leq0.036$). For p16+ cell quantification, a total of 187±55 and 178±56 fibers were counted prior to the eight weeks and 204±55 and 203±69 fibers after eight weeks for the trained and untrained legs, respectively. The Friedman test was conducted for the total number of p16+ cells in MA participants and showed that there was a significant effect between legs ($p=0.002$, Fig. 3c). A Wilcoxon test indicated that these cells were significantly

greater after training compared to the pre-training values in the trained leg (p=0.035). A Friedman test was also conducted to assess p16+ satellite cells (p16+/Pax7+) across legs in MA participants. The test yielded a significant result (trained leg: 0.42±0.91 to 1.07±1.34 cells/100 fibers; untrained leg: 0.90±1.28 to 1.47±1.55 cells/100 fibers, p<0.001, Fig. 3f), and a Wilcoxon test indicated that these cells were significantly greater after training compared to the pre-training values in the trained leg (p=0.015). At no time or leg was there a significant difference between MA and Y participants for this phenotype.

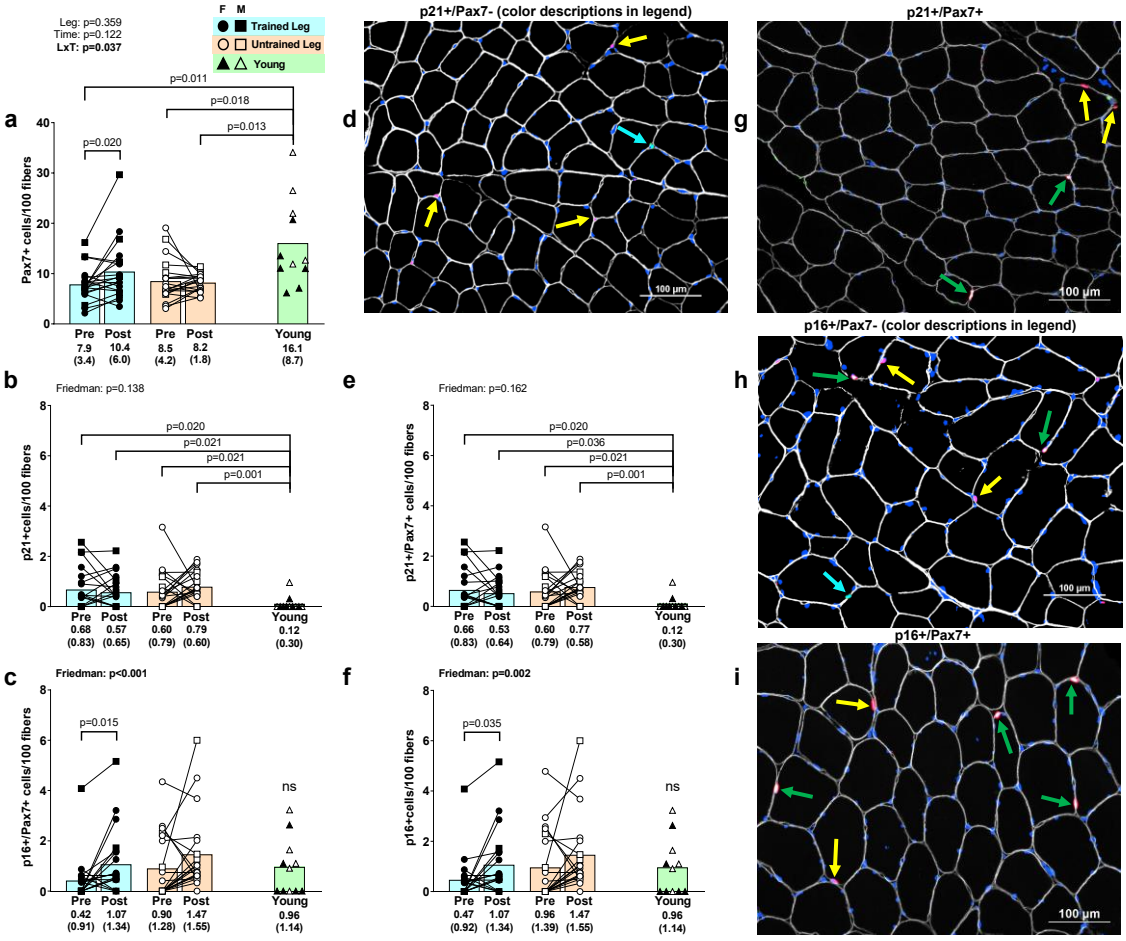

Figure 3. Satellite cells and senescent cells

Legend: Variables presented include Pax7+ cells per 100 fibers (a), p21+ cells/100 fibers (b), p21+/Pax7+ (satellite) cells/100 fibers (e), p16+ cells/100 fibers (c), and p16+/Pax7+ (satellite) cells/100 fibers. Graphs contain n=20 middle-aged (MA) participants (55±8 years old, n=15 females, n=5 males) and n=11 Y participants (23±4 years old, n=6 females, n=5 males). Data are

presented as mean ± standard deviation values for PRE and POST MA-trained and MA-untrained leg, and the Y comparator group. Individual responses are also illustrated, with open circles and squares indicating females and males, respectively, for the MA-untrained leg and closed circles and squares indicating females and males, respectively, for the MA-trained leg. Open and closed triangles indicate Y females and males, respectively. Representative images are presented in panels d, and g-i. Target colors in images are as follows: dystrophin (gray, pseudo color), Pax7 (red), DAPI (blue), and p21 or p16 (green). Arrows in images are as follows: p21-/Pax7+cells (yellow arrow), p21+ and Pax7-cells (cyan arrow), and p21+/Pax7+ cells (green arrow) in panels d and g, and p16-/Pax7+cells (yellow arrow), p16+ and Pax7-cells (cyan arrow), and p16+/Pax7+ cells (green arrow) in panels h and i.

Given the high number of p16+ and p21+ cells that co-localized with Pax7, we opted to provide a depiction of the percentage of senescent cells that were satellite cells (and vice versa) for Y and MA participants (trained leg only) (Fig. 4). Interestingly, while >90% satellite cells were not p16+ or p21+, most of the p16+ and p21+ cells co-localized with Pax7 (>90% on average in both MA time points and Y) indicating that most of the senescent cells were satellite cells in both age cohorts.

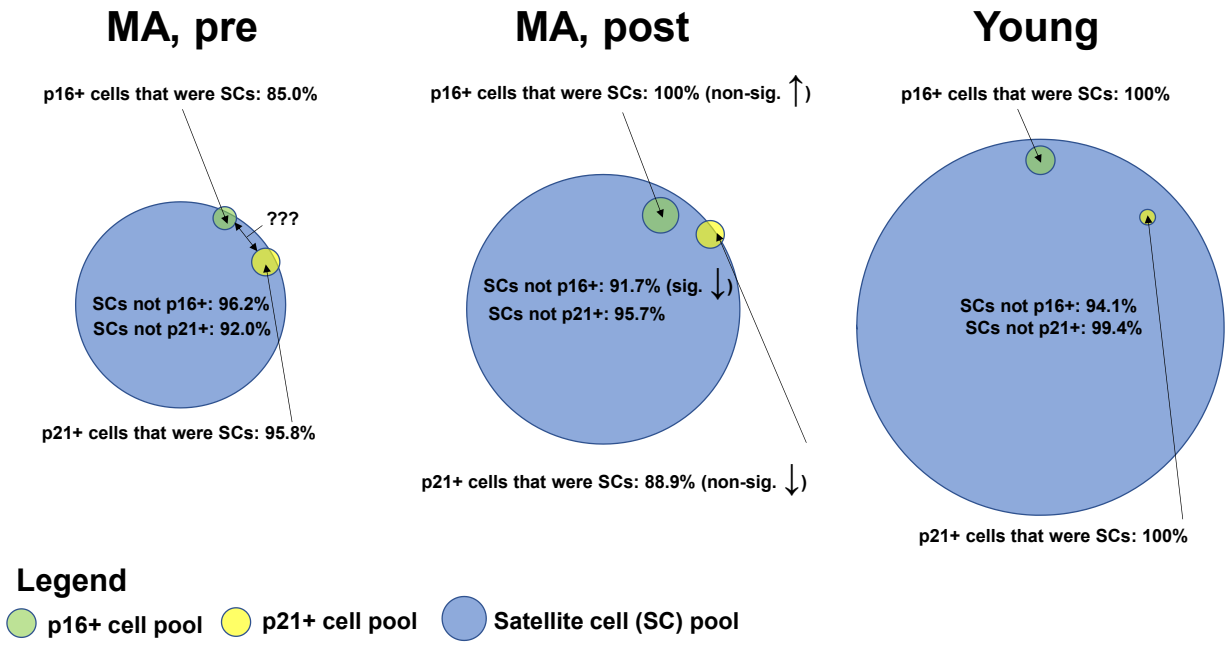

Figure 4. Percentage of satellite cells that were senescent cells and vice versa
Legend: Figure contains average cell percentages from the trained leg of n=20 middle-aged (MA) participants (55±8 years old, n=15 females, n=5 males) and n=11 Y participants (23±4 years old, n=6 females, n=5 males). Note: ???, indicates that the percentage of p16+ and p21+ cell overlap is unknown given that this stain was not performed due to the limited number of filters utilized.

Potential Sex Differences

While the number of male participants was small, we did perform exploratory *post hoc* three-way repeated measures ANOVAs on VL mCSA, leg extensor peak torque and histology outcomes (NCAM+ fibers, fCSAs, satellite cells, p16+/p21+ cells) to examine whether any sex-specific differences existed. The only significant interaction was a leg-by-time-by-sex interaction for percent type II NCAM+ myofibers in the trained leg only whereby PRE to POST change scores were lower in MA females versus males (females: -0.32±1.38%, males: 2.71±2.88%; p=0.014). Notably, these comparisons were not performed for proteomics or the SASP protein array data given that data from fewer than 5 males were available for those variables.

Changes in sarcoplasmic proteins related to muscle-nerve communication

The sarcoplasmic proteins related to muscle-nerve interaction are shown in Table 3. Of the 47 proteins, 13 significantly changed with training (all upregulated), 18 were significantly different prior to training compared to the Y cohort, and 20 were significantly different after training compared to the Y cohort.

Table 3. Expression of sarcoplasmic proteins related to muscle-nerve communication

Gene name	Protein name	MA PRE	MA POST	Y
Denervation				
NCAM1	Neural Cell adhesion molecule	4.9±2.6	6.8±4.0*	5.6±6.6
HDAC4	Histone deacetylase 4	6.3±1.6	10.5±4.6*	6.4±2.2†
CASQ1	Calsequestrin-1	2219±711	1949±705	1261±292$^{\#\dagger}$
NEDD4	E3 ubiquitin-protein ligase NEDD4	13.2±2.6	14.6±3.6	12.7±2.5

DAG1	Dystroglycan 1	13.7±3.2	14.4±4.7	12.4±3.3
SGCA	Alpha-sarcoglycan	26.1±5.3	26.5±8.5	27.4±7.3
DMD	Dystrophin	18.2±5.3	16.5±4.9	16.9±4.7
FBXO30	F-box only protein 30	0.6±0.3	1.0±0.4*	0.7±0.4
FBXO40	F-box only protein 40	3.8±1.4	3.6±1.3	2.6±1.0#†
FBXO21	F-box only protein 21	2.5±0.7	2.6±0.7	1.6±0.4#†
NES	Nestin	5.1±1.1	6.6±2.3*	4.9±2.0
Neuromuscular Junction				
DLGAP4	Disks large-associated protein 4	7.7±2.2	8.0±2.4	6.1±1.2
CD2AP	CD2-associated protein	5.9±2.0	7.1±2.0	5.8±1.5
DES	Desmin	99.6±16.7	99.4±28.5	80.1±20.8#
PRKACA	cAMP-dependent protein kinase catalytic subunit alpha	80.6±29.4	68.0±32.1	101±27†
DLG1	Disks large homolog 1	5.3±1.9	5.8±1.6	3.6±0.9#
CRKL	Crk-like protein	53.1±11.4	64.7±18.0*	57.0±11.3
CRK	Adapter molecule crk	7.6±1.9	10.4±2.6*	8.0±1.6†
ANK3	Ankyrin-3	15.1±4.6	13.8±3.6	9.2±2.8#†
LAMB2	Laminin subunit beta-2	9.1±3.2	11.7±5.0	10.0±4.5
CDH15	Cadherin-15	11.2±3.0	12.3±3.5	9.4±2.2†
ACHE	Acetylcholinesterase	2.1±0.7	2.4±1.0	1.5±0.5#†
UTRN	Utrophin	1.6±0.4	2.1±0.6*	1.5±0.4†
PRKAR1A	cAMP-dependent protein kinase type I-alpha regulatory subunit	117±39	116±53	88.3±34.1#
SNTA1	Alpha-1-syntrophin	33.0±7.7	34.0±13.2	32.7±7.6
Neuromuscular Junction Development				
FNTA	Protein farnesyltransferase/ geranylgeranyltransferase type-1 subunit alpha	7.9±2.7	12.3±3.5*	11.4±1.7#
GPHN	Gephyrin	18.0±4.2	18.8±5.7	14.5±2.5#†
DOK7	Docking Protein 7	9.3±3.6	9.6±3.0	7.8±2.2
AGRN	Agrin	1.6±0.6	1.9±0.8	1.8±0.8
CACNA1S	Voltage-dependent L-type calcium channel subunit alpha-1S	44.6±15.9	49.3±21.4	32.9±10.4†
CACNB3	Voltage-dependent L-type calcium channel subunit beta-3	18.0±5.6	17.1±5.3	15.1±1.9
DCTN1	Dynactin subunit 1	34.1±7.2	38.8±11.2	26.4±6.5#†
Innervation				
LRIG1	Leucine-rich repeats and immunoglobulin-like domains protein 1	0.8±0.3	0.9±0.4	0.8±0.2
NRP1	Neuropilin-1	3.1±1.1	4.7±1.8*	3.7±1.6
Skeletal muscle tissue regeneration				
PPP3CA	Protein phosphatase 3 catalytic subunit alpha	27.4±5.7	32.1±11.6	30.0±7.3
KPNA1	Importin subunit alpha-5	56.4±10.7	59.2±16.4	54.3±11.3
MTPN	Myotrophin	2.6±1.6	7.4±13.8*	5.8±4.2#
GPX1	Glutathione peroxidase 1	83.8±47.1	83.2±47.0	34.5±15.3#†
CD81	CD81 antigen	14.6±3.7	14.1±4.4	10.4±2.8#†
ANXA1	Annexin A1	7.4±3.5	6.2±4.3	4.5±2.2#
Axon Regeneration				
TSPO	Translocator protein	456±201	433±274	197±87#†
MAP1B	Microtubule-associated protein 1b	5.3±1.4	7.8±3.3*	6.6±3.9
GRN	Progranulin	1.9±0.9	2.6±1.5	1.2±0.8#†

Axon Guidance				
TUBB3	Tubulin beta-3 chain	2.1±0.7	3.5±1.6*	2.0±0.8†
MYPN	Myopalladin	7.6±2.4	8.6±2.7	5.4±1.6$^{\#\dagger}$
CDK5	Cyclin-dependent kinase 5	11.3±1.7	14.7±3.6*	11.6±3.6†

Legend: Values for proteins of interest are presented as mean ± standard deviation values for 18 middle-aged (MA) participants (trained leg only) and 9 younger (Y) participants. Symbols: *, indicates a significant difference ($p<0.05$) from PRE to POST with in MA participants; $^{\#}$, indicates a significant difference between MA participants at PRE and Y participants; †, indicates a significant difference between MA participants at POST and Y participants.

Changes in sarcoplasmic proteins related to cellular senescence

There were 15 proteins of interest related to "cellular senescence" that were identified (Fig. 5). Eight of the 15 proteins were significantly altered with training (MAP2K1: 38.5±11.6 to 49.7±20.7, p=0.048; MAP2K3: 68.7±15.4 to 94.7±32.3, p=0.006; MAP2K4: 11.3±2.0 to 13.8±3.9, p=0.031; MAP2K6: 33.6± 8.1 to 51.3±25.5, p=0.012; MIF: 27.9±11.0 to 18.1±7.4, p=0.004; GLB1: 1.6±0.5 to 2.4±1.3, p=0.006; DNAJA3: 14.3±6.8 to 17.5±6.7, p=0.026; PML: 3.4±0.8 to 4.0±1.2, p=0.034). Prior to training, 6 of the 15 proteins were significantly different in MA versus Y participants (MAP2K1: 38.5±11.6 versus 62.3±18.1, p<0.001; MAPK14: 20.5±5.4 versus 30.4±7.8, p<0.001; NPM1: 36.0±15.9 versus 14.8±7.3, p<0.001; NUP62: 5.2±2.5 versus 3.2±0.9, p=0.014; DNAJA3: 14.3±6.8 versus 9.4±3.9, p=0.040). After training, 6 of the 15 proteins were significantly in MA versus Y participants (MAP2K6: 51.3±25.5 versus 32.4±7.5, p=0.035; NPM1: 39.2±18.3 versus 14.8±7.3, p<0.001; NUP62: 5.2±1.4 versus 3.2±0.9, p=0.001; CALR: 137±35 versus 113±18, p=0.026; DNAJA3: 17.5±6.7 versus 9.4±3.9, p=0.003; PML: 4.0±1.2 versus 3.1±0.5, p=0.025). Lastly, two search terms "Replicative senescence" and "Positive regulation of cellular senescence", were not included in Figure 4, but are shown in Table 3 below.

To further interrogate whether cellular senescence was upregulated with training, we entered the seven proteins from the "cellular senescence" pathway that were upregulated, into

PANTHER pathway analysis (MAP2K1, MAP2K3, MAP2K4, MAP2K6, GLB1, DNAJA3, PML) [208] and performed the PANTHER Overrepresentation Test whereby Fisher's Exact and False Discovery Rate was calculated [209]. The test indicated that "cellular senescence" was predicted to be >100-fold upregulated (raw p-value = 5.99 x 10^{-15}, FDR = 9.35 x 10^{-11}).

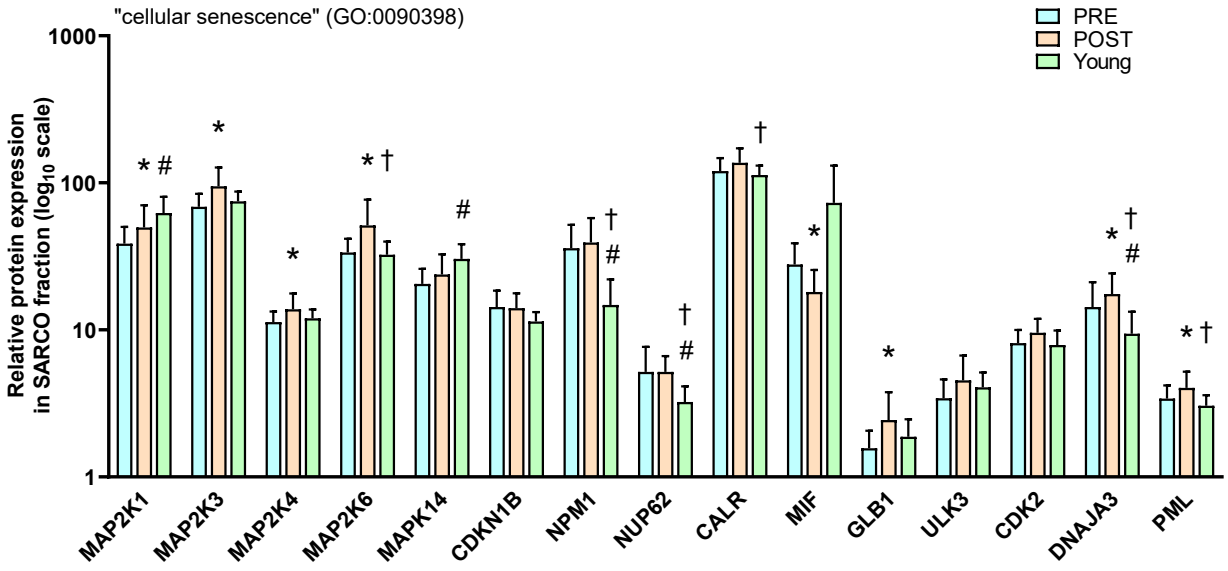

Figure 5. Expression of sarcoplasmic proteins related to cellular senescence
Legend: Data presented as mean ± standard deviation values from n=18 middle-aged (MA) participants (55±8 years old, n=14 females, n=4 males) and n=9 Y participants (22±2 years old, n=7 females, n=2 males). Data are scaled as $\log_{10}$ values to improve visualization. Symbols: *, indicates a significant difference ($p<0.05$) from PRE to POST in MA participants; $^{\#}$, indicates a significant difference between MA participants at PRE and Y participants; †, indicates a significant difference between MA participants at POST and Y participants.

Table 4. Expression of other sarcoplasmic proteins related cellular senescence

Gene name	Protein name	MA PRE	MA POST	Y
Replicative senescence				
MME	Neprilysin	15.9±6.6	18.4±5.5	23.2±12.3$^{\#}$
ROMO1	Reactive oxygen species modulator 1	423±201	388±238	148±55$^{\#\dagger}$
Positive regulation of cellular senescence				
EEF1E1	Eukaryotic translation elongation factor 1 epsilon-1	4.2±1.1	5.5±2.1*	3.1±1.1$^{\#\dagger}$
B2M	Beta-2-microglobulin	5.4±2.3	7.3±3.0*	3.8±1.0†

Legend: Data presented as mean ± standard deviation values from n=18 middle-aged (MA) participants (55±8 years old, n=14 females, n=4 males) and n=9 younger participants (22±2

years old, n=7 females, n=2 males). Symbols: *, indicates a significant difference ($p<0.05$) from PRE to POST in MA participants; #, indicates a significant difference between MA participants at PRE and younger (Y) participants; †, indicates a significant difference between MA participants at POST and Y participants.

Changes in SASP protein expression

Based on comprehensive reviews [210, 211], 17 of the 160 targets provided by the antibody array were interrogated as SASP targets of interest (MCP-1, Osteopontin, IL-1α/-6/-8/-10, GM-CSF, GRO-a, IFN-g, MCSF, RANTES, HGF, IGFBP3/4, TGFβ1/2, and VEGF; Figure 6). One of the 17 SASP proteins were significantly altered with training in MA participants (IGFBP-3: 0.546±1.076 to 1.257±2.024, p=0.031). Prior to training, no SASP proteins were significantly different in MA versus Y participants. After training, two of the 17 SASP proteins were significantly different in MA versus Y participants (IGFBP-3: 1.257±2.024 versus 0.091±0.204, respectively; p=0.048; Osteopontin: 1.253±1.636 versus 0.185±0.258, respectively; p=0.025).

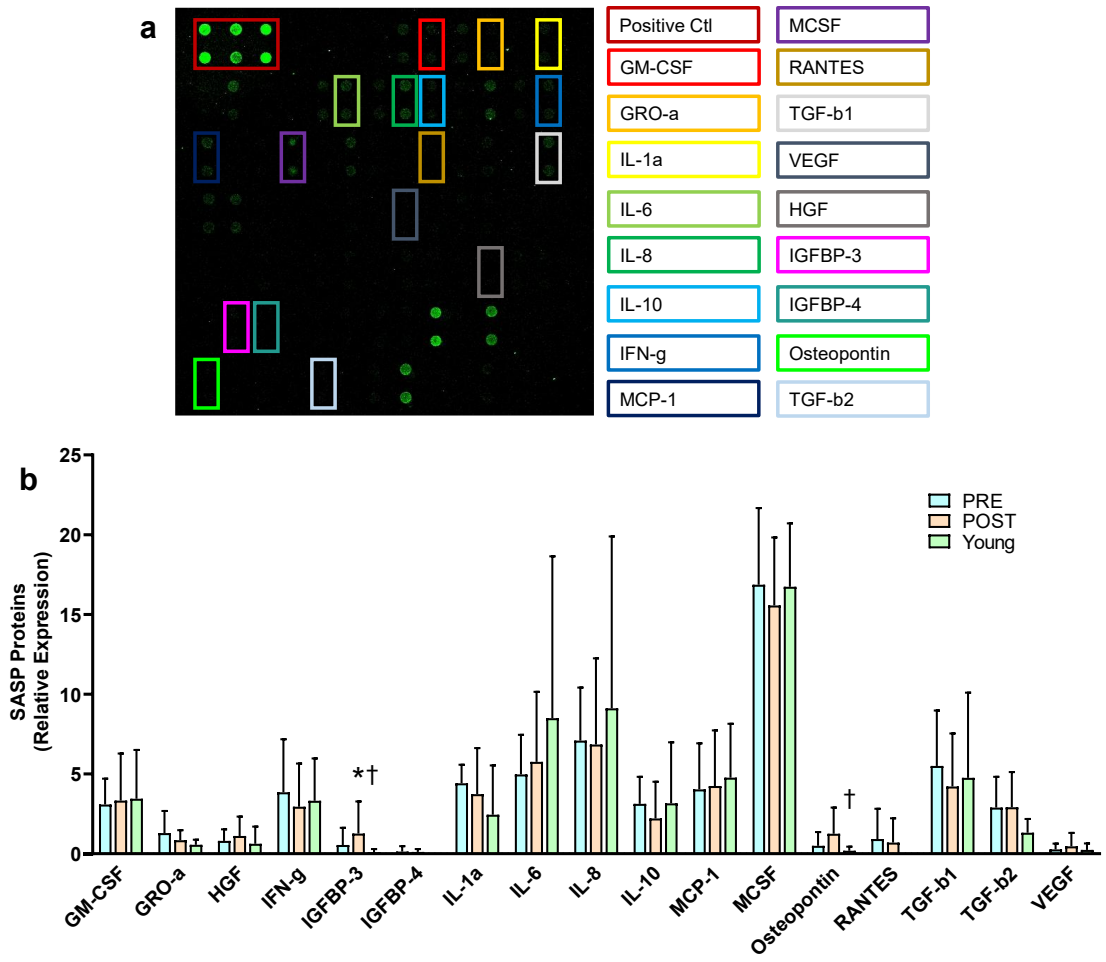

Figure 6. Expression of SASP proteins
Legend: (a) A representative array, where each sample was assayed in duplicate. The level of SASP protein expression is proportional to fluorescence intensity. SASP proteins are labeled and color matched on the right. (b) SASP protein expression data presented from n=13 MA participants (58±8 years old, n=3 males, n=10 females) and n=5 Y participants (22±1 years old, n=1 males, n=4 females). Symbols: *, indicates a significant difference ($p<0.05$) from PRE to POST in MA participants; †, indicates a significant difference between MA participants at POST and Y participants.

DISCUSSION

We sought to examine if denervated myofibers, senescent cells, and associated protein markers in MA individuals were affected with eight weeks of unilateral knee extensor resistance training, and whether training restores these markers to "youth-like" levels. Our primary findings are as follows: i) despite age-related differences in denervated myofiber content, resistance

training did not affect this variable, ii) training did not alter p16+ and p21+ cell content or most SASP proteins, albeit training did increase several senescence-associated proteins, iii) training increased satellite cell content in the absence of myofiber hypertrophy, iv) there were more p21+ cells in MA compared with Y participants, and v) although most satellite cells were not senescent, most senescent cells were satellite cells. Finally, the applied and cellular responses seemed to be largely conserved between sexes, albeit limited sample sizes for males require more validation research in this regard.

The current literature is mixed as to whether exercise training can affect NCAM+ myofibers in older adults. Our null findings in the current study are congruent with other studies [16, 18], albeit one study has indicated that the area occupied by NCAM+ myofibers in muscle sections is reduced with resistance training [17]. Although we did not observe a training effect, it is interesting that the percentage of mixed and type I NCAM+ fibers were significantly greater at PRE in the trained leg of MA versus Y participants. Further, unlike PRE values, values of NCAM+ myofibers (both total and type I) in the trained leg at POST were not significantly different from the Y cohort. Also notable, several proteins related to muscle-nerve communication were upregulated in the trained leg of MA participants. We interpret these collective findings to suggest that, had the training intervention been longer or perhaps more intense, resistance training may have increased type I (but not type II) fiber innervation. This is a plausible hypothesis given that various reports indicate that active, MA individuals possess larger type I fibers relative to inactive counterparts while also possessing a greater degree of fiber type grouping, alluding to a greater degree of reinnervation [10, 142]. However, Soendenbroe et al. [18] recently reported that a training intervention that was twice as long in duration compared to the current study and had participants perform two additional leg exercises

per session did not affect the number of NCAM+ fibers. Hence, it is currently unclear how shorter-term resistance training affects myofiber denervation, and more studies in both middle-aged and older participants are needed to draw more definitive conclusions.

Senescent cell number has been reported to be higher in aged skeletal muscle [204], and recent research interest has investigated how exercise affects this phenotype [212, 213]. While numerous studies have shown a decrease in senescent markers with exercise [22, 23, 214-216], our results suggest training does not affect p16+ or p21+ cells in skeletal muscle. There was an age effect with p21+ satellite cells whereby the MA participants had a significantly higher abundance compared to the younger cohort in both legs prior to and following the training intervention. Past reports have indicated that senescent cells are not altered or increase with mechanical overload [217-219]. However, it is noteworthy that studies examining p16+ or p21+ senescent cells with exercise have not indicated whether they are satellite cells. A key finding in our investigation is that most senescent cells co-localized with Pax7 in both age cohorts. Additionally, satellite cells increased in the trained leg, and this coincided with several senescent-related proteins increasing in the trained leg as well. Another interesting and related finding is that SASP proteins did not increase in the trained leg of MA participants despite several senescent proteins increasing, and SASP protein differences between MA and Y were marginal despite p21+ cells being higher in both legs of MA at all times. While speculative, we interpret this collective evidence to suggest that senescence signals in muscle tissue could primarily come from satellite cells, and that the increase in satellite cells observed with training drove several of the senescence-related protein (but not SASP protein) responses. This viewpoint is partially supported by a recent review [213] indicating that the expression of cyclin-dependent kinase inhibitors and other cellular senescence proteins could generally represent an increase in

cell proliferation and differentiation rather than cellular senescence. This hypothesis may also, in part, explain why Dungan and colleagues reported a robust increase in p21+ cells 14 days following an acute resistance exercise bout in younger (21-39-year-old) participants [25]. Specifically, while the authors did not examine if these cells co-localized with Pax7, it remains possible that the increase in p21+ and SA β-Gal cells were a portion of the satellite cell pool that were primed for differentiation.

It is worth discussing the satellite cell findings in the context of other training adaptations observed in the present investigation. While there are disagreements in the literature about how aging affects satellite cells [31-33, 88, 89, 220], the current data indicate MA individuals had fewer satellite cells than younger individuals prior to training. With training, however, MA participants were able to increase satellite cell numbers back to youth-like levels, albeit this was not accompanied with increases in fCSA or myonuclear number. Other studies have demonstrated similar increases in satellite cell content with resistance training in MA participants, but with mixed hypertrophic outcomes [221, 222]. It has been previously reported that satellite cell content prior to training (regardless of age) is linked to different hypertrophy outcomes, which could explain the lack of myofiber hypertrophy in the current study [91, 223]. In addition to the lack of fCSA increases with training, the lower number of satellite cells prior to training in MA versus younger participants could explain why fCSA, specifically type II fCSA, was lower in the MA participants. While we did not interrogate fiber-type specific satellite cell content, others have shown that older participants possess significantly less type II fiber-specific satellite cells which corresponds with smaller type II fCSA [34, 222, 224]. It should also not be discounted that, while myofiber hypertrophy was not observed in the trained leg of MA participants, the increase in satellite cells could have acted to facilitate other adaptations (e.g.,

connective tissue remodeling) as reported in murine models by Fry and colleagues [225, 226], and this could have acted to facilitate tissue-level hypertrophy. Notwithstanding, the current data supports that satellite cells increase with resistance training and, had training been longer or more rigorous, this may have eventually translated to an increase in myofiber hypertrophy.

A final topic worthy of discussion is the paradoxical findings between VL mCSA changes in MA participants' trained leg (which trended upward) and the numerical decreases in fCSA values. We have observed this phenomenon on prior occasions with resistance training interventions [195, 227], and speculate that this is likely due to the limited number of myofibers sampled with histology. However, it is intriguing that fCSA values numerically decreased given that our past studies suggested that tissue-level and myofiber area increases, while not significantly associated, both directionally increase with resistance training. Although this is difficult to reconcile, we posit that this may be due to the mild nature of knee extensor-only resistance training. Alternatively stated, relatively modest training adaptations were observed, and it is likely that more robust adaptations would have been observed had participants performed multiple exercises targeting the knee extensor muscles (e.g., knee extensors, squats, deadlifts, etc.).

Limitations

Our study was not without limitations. First, we pooled MA participants who consumed a nutritional supplement or placebo over the eight-week intervention. As stated, the resistance training arm of this protocol was designed to examine the current research question, and we had no reason to suspect that the outcome variables in the trained leg would be affected by the supplied supplementation. While we provided evidence of this in the methods section, readers

should be aware of this study design limitation. It is also worth noting that proteomic data were obtained from tissue containing mixed myofibers and stromal cells. Single fiber (or single cell) isolation with downstream proteomics analysis for NCAM+ fiber-specific, or p16+/p21+ cell-specific protein expression profiles would have provided more insight as to how training affected the proteins of interest in a cell-specific fashion. Additionally, the training paradigm we implemented was isolated to a single leg, and results may have differed had multiple leg exercises or full body training been implemented. Having a younger cohort that trained would have also been beneficial to examine whether the training adaptations seen with the MA participants were similar in younger participants. Lastly, there were a limited number of male participants in the study which limited our power to determine whether sex-specific adaptations existed in MA participants.

Conclusions

In summary, although eight weeks of unilateral leg resistance training did not affect denervated myofiber or p16+/p21+ senescent cell counts in MA individuals, several proteins associated with muscle-nerve communication and senescence were upregulated. We conclude that resistance training either: i) needed to be more vigorous and/or longer in duration to eventually affect these outcomes, or ii) does not affect these outcomes. Hence, more research is needed in this regard to provide further clarity. We also provide continued support for the role of resistance training in increasing satellite cell numbers in MA participants. Finally, most p16+/p21+ senescent cells in the muscle tissue of younger and MA participants were Pax7+ satellite cells, and SASP proteins were generally not different between MA and Y participants. Thus, we posit that these signatures represent the existence of a subpopulation of satellite cells,

rather than proinflammatory SASP-secreting cells, being the primary source of senescent-like cells in skeletal muscle.

ACKNOWLEDGEMENTS

We thank the participants who volunteered and participated in the study. We thank Seer, Inc. and their team members (David Hill, Mara Riley, Ryan Hill, Aaron S. Gajadhar, and others) for assisting us through the various procedures needed to perform proteomics analysis including performing pilot feasibility experiments using the Proteograph Product Suite. Shao-Yung Chen is an employee of Seer, Inc. who was largely responsible for the execution of the pilot feasibility experiments, although he had no role in the study design. The study design and outcome variables of this pooled analysis sought to examine training outcomes unrelated to the nutritional supplement administered herein, and the study design was created by B.A.R. and M.D.R. to fulfill dissertation requirements for B.A.R. However, the reader should be aware that M.D.R. and T.N.Z. have published research examining the effects of the administered supplement on unrelated cellular metabolites and metabolic enzymes *in vitro* and in humans, and current exploratory analyses from blood specimens and tissue specimens from the untrained leg of MA participants are ongoing in this regard. None of the other co-authors have apparent conflicts of interest in relation to these data.

DATA AVAILABILITY

Raw data related to the current study outcomes will be provided upon reasonable request by emailing the corresponding author.

FUNDING INFORMATION

Funding for participant compensation, histology, and proteomics was made possible through gift and discretionary funds from the M.D.R. laboratory, discretionary funds from the A.D.F. laboratory, and indirect cost sharing (generated from various unrelated contracts) from the School of Kinesiology. M.C.M. was fully supported through a T32 NIH grant (T32GM141739), and D.L.P. was fully supported by a Presidential Graduate Research Fellowship funded by Auburn University's President's office, the College of Education, and School of Kinesiology.

REFERENCES

1. Frontera, W.R. and J. Ochala, *Skeletal muscle: a brief review of structure and function.* Calcif Tissue Int, 2015. **96**(3): p. 183-95.
2. Rudolf, R., et al., *Degeneration of neuromuscular junction in age and dystrophy.* Front Aging Neurosci, 2014. **6**: p. 99.
3. Hepple, R.T. and C.L. Rice, *Innervation and neuromuscular control in ageing skeletal muscle.* J Physiol, 2016. **594**(8): p. 1965-78.
4. Brown, M.C., R.L. Holland, and W.G. Hopkins, *Motor nerve sprouting.* Annu Rev Neurosci, 1981. **4**: p. 17-42.
5. Soendenbroe, C., J.L. Andersen, and A.L. Mackey, *Muscle-nerve communication and the molecular assessment of human skeletal muscle denervation with aging.* Am J Physiol Cell Physiol, 2021. **321**(2): p. C317-C329.
6. Aare, S., et al., *Failed reinnervation in aging skeletal muscle.* Skelet Muscle, 2016. **6**(1): p. 29.
7. Jones, E.J., et al., *Ageing and exercise-induced motor unit remodelling.* J Physiol, 2022. **600**(8): p. 1839-1849.
8. Cruz-Jentoft, A.J. and A.A. Sayer, *Sarcopenia.* Lancet, 2019. **393**(10191): p. 2636-2646.
9. Soendenbroe, C., et al., *Key Components of Human Myofibre Denervation and Neuromuscular Junction Stability are Modulated by Age and Exercise.* Cells, 2020. **9**(4).
10. Sonjak, V., et al., *Fidelity of muscle fibre reinnervation modulates ageing muscle impact in elderly women.* J Physiol, 2019. **597**(19): p. 5009-5023.
11. Lai, X., et al., *Effects of lower limb resistance exercise on muscle strength, physical fitness, and metabolism in pre-frail elderly patients: a randomized controlled trial.* BMC Geriatr, 2021. **21**(1): p. 447.
12. Charette, S.L., et al., *Muscle hypertrophy response to resistance training in older women.* J Appl Physiol (1985), 1991. **70**(5): p. 1912-6.
13. Pyka, G., et al., *Muscle strength and fiber adaptations to a year-long resistance training program in elderly men and women.* J Gerontol, 1994. **49**(1): p. M22-7.
14. Ivey, F.M., et al., *Effects of strength training and detraining on muscle quality: age and gender comparisons.* J Gerontol A Biol Sci Med Sci, 2000. **55**(3): p. B152-7; discussion B158-9.
15. Treuth, M.S., et al., *Effects of strength training on total and regional body composition in older men.* J Appl Physiol (1985), 1994. **77**(2): p. 614-20.
16. Voigt, T.B., et al., *Resistance training-induced gains in knee extensor strength are related to increased neural cell adhesion molecule expression in older adults with knee osteoarthritis.* BMC Res Notes, 2019. **12**(1): p. 595.
17. Messi, M.L., et al., *Resistance Training Enhances Skeletal Muscle Innervation Without Modifying the Number of Satellite Cells or their Myofiber Association in Obese Older Adults.* J Gerontol A Biol Sci Med Sci, 2016. **71**(10): p. 1273-80.
18. Soendenbroe, C., et al., *Human skeletal muscle acetylcholine receptor gene expression in elderly males performing heavy resistance exercise.* Am J Physiol Cell Physiol, 2022. **323**(1): p. C159-C169.
19. Brightwell, C.R., et al., *Moderate-intensity aerobic exercise improves skeletal muscle quality in older adults.* Transl Sports Med, 2019. **2**(3): p. 109-119.

20. Straight, C.R., et al., *Improvements in skeletal muscle fiber size with resistance training are age-dependent in older adults: a systematic review and meta-analysis.* J Appl Physiol (1985), 2020. **129**(2): p. 392-403.
21. Ben-Porath, I. and R.A. Weinberg, *The signals and pathways activating cellular senescence.* Int J Biochem Cell Biol, 2005. **37**(5): p. 961-76.
22. Yoon, K.J., et al., *Exercise-induced AMPK activation is involved in delay of skeletal muscle senescence.* Biochem Biophys Res Commun, 2019. **512**(3): p. 604-610.
23. Rossman, M.J., et al., *Endothelial cell senescence with aging in healthy humans: prevention by habitual exercise and relation to vascular endothelial function.* Am J Physiol Heart Circ Physiol, 2017. **313**(5): p. H890-H895.
24. Childs, B.G., et al., *Senescent cells: an emerging target for diseases of ageing.* Nat Rev Drug Discov, 2017. **16**(10): p. 718-735.
25. Dungan, C.M., et al., *Senolytic treatment rescues blunted muscle hypertrophy in old mice.* Geroscience, 2022. **44**(4): p. 1925-1940.
26. Allen, D.L., R.R. Roy, and V.R. Edgerton, *Myonuclear domains in muscle adaptation and disease.* Muscle Nerve, 1999. **22**(10): p. 1350-60.
27. Zammit, P.S., T.A. Partridge, and Z. Yablonka-Reuveni, *The skeletal muscle satellite cell: the stem cell that came in from the cold.* J Histochem Cytochem, 2006. **54**(11): p. 1177-91.
28. Hikida, R.S., *Aging changes in satellite cells and their functions.* Curr Aging Sci, 2011. **4**(3): p. 279-97.
29. Hawke, T.J. and D.J. Garry, *Myogenic satellite cells: physiology to molecular biology.* J Appl Physiol (1985), 2001. **91**(2): p. 534-51.
30. Murach, K.A., et al., *Myonuclear Domain Flexibility Challenges Rigid Assumptions on Satellite Cell Contribution to Skeletal Muscle Fiber Hypertrophy.* Front Physiol, 2018. **9**: p. 635.
31. Sajko, S., et al., *Frequency of M-cadherin-stained satellite cells declines in human muscles during aging.* J Histochem Cytochem, 2004. **52**(2): p. 179-85.
32. Renault, V., et al., *Regenerative potential of human skeletal muscle during aging.* Aging Cell, 2002. **1**(2): p. 132-9.
33. Verdijk, L.B., et al., *Satellite cells in human skeletal muscle; from birth to old age.* Age (Dordr), 2014. **36**(2): p. 545-7.
34. Verdijk, L.B., et al., *Satellite cell content is specifically reduced in type II skeletal muscle fibers in the elderly.* Am J Physiol Endocrinol Metab, 2007. **292**(1): p. E151-7.
35. Sousa-Victor, P., et al., *Geriatric muscle stem cells switch reversible quiescence into senescence.* Nature, 2014. **506**(7488): p. 316-21.
36. Chakkalakal, J.V., et al., *The aged niche disrupts muscle stem cell quiescence.* Nature, 2012. **490**(7420): p. 355-60.
37. Dreyer, H.C., et al., *Satellite cell numbers in young and older men 24 hours after eccentric exercise.* Muscle Nerve, 2006. **33**(2): p. 242-53.
38. Conboy, I.M., et al., *Notch-mediated restoration of regenerative potential to aged muscle.* Science, 2003. **302**(5650): p. 1575-7.
39. Masters, T.A., J. Kendrick-Jones, and F. Buss, *Myosins: Domain Organisation, Motor Properties, Physiological Roles and Cellular Functions.* Handb Exp Pharmacol, 2017. **235**: p. 77-122.

40. Steffen, W., et al., *Mapping the actin filament with myosin.* Proc Natl Acad Sci U S A, 2001. **98**(26): p. 14949-54.
41. Glancy, B. and R.S. Balaban, *Energy metabolism design of the striated muscle cell.* Physiol Rev, 2021. **101**(4): p. 1561-1607.
42. Staron, R.S., *Human skeletal muscle fiber types: delineation, development, and distribution.* Can J Appl Physiol, 1997. **22**(4): p. 307-27.
43. Schiaffino, S. and C. Reggiani, *Fiber types in mammalian skeletal muscles.* Physiol Rev, 2011. **91**(4): p. 1447-531.
44. Johnson, M.A., et al., *Data on the distribution of fibre types in thirty-six human muscles. An autopsy study.* J Neurol Sci, 1973. **18**(1): p. 111-29.
45. Costill, D.L., et al., *Skeletal muscle enzymes and fiber composition in male and female track athletes.* J Appl Physiol, 1976. **40**(2): p. 149-54.
46. Gollnick, P.D., et al., *Effect of training on enzyme activity and fiber composition of human skeletal muscle.* J Appl Physiol, 1973. **34**(1): p. 107-11.
47. Lexell, J., *Human aging, muscle mass, and fiber type composition.* J Gerontol A Biol Sci Med Sci, 1995. **50 Spec No**: p. 11-6.
48. Lexell, J., C.C. Taylor, and M. Sjostrom, *What is the cause of the ageing atrophy? Total number, size and proportion of different fiber types studied in whole vastus lateralis muscle from 15- to 83-year-old men.* J Neurol Sci, 1988. **84**(2-3): p. 275-94.
49. Plotkin, D.L., et al., *Muscle Fiber Type Transitions with Exercise Training: Shifting Perspectives.* Sports (Basel), 2021. **9**(9).
50. Jansson, E. and L. Kaijser, *Muscle adaptation to extreme endurance training in man.* Acta Physiol Scand, 1977. **100**(3): p. 315-24.
51. Fry, A.C., et al., *Muscle fiber characteristics and performance correlates of male Olympic-style weightlifters.* J Strength Cond Res, 2003. **17**(4): p. 746-54.
52. Kosek, D.J., et al., *Efficacy of 3 days/wk resistance training on myofiber hypertrophy and myogenic mechanisms in young vs. older adults.* J Appl Physiol (1985), 2006. **101**(2): p. 531-44.
53. Gesslbauer, B., et al., *Axonal components of nerves innervating the human arm.* Ann Neurol, 2017. **82**(3): p. 396-408.
54. Tomlinson, B.E. and D. Irving, *The numbers of limb motor neurons in the human lumbosacral cord throughout life.* J Neurol Sci, 1977. **34**(2): p. 213-9.
55. Feinstein, B., et al., *Morphologic studies of motor units in normal human muscles.* Acta Anat (Basel), 1955. **23**(2): p. 127-42.
56. Gath, I. and E. Stalberg, *In situ measurement of the innervation ratio of motor units in human muscles.* Exp Brain Res, 1981. **43**(3-4): p. 377-82.
57. Burke, R.E. and P. Tsairis, *Anatomy and innervation ratios in motor units of cat gastrocnemius.* J Physiol, 1973. **234**(3): p. 749-65.
58. Burke, R.E., *Motor unit types of cat triceps surae muscle.* J Physiol, 1967. **193**(1): p. 141-60.
59. Gardiner, P.F. and D. Kernell, *The "fastness" of rat motoneurones: time-course of afterhyperpolarization in relation to axonal conduction velocity and muscle unit contractile speed.* Pflugers Arch, 1990. **415**(6): p. 762-6.
60. Plomp, J.J., *Trans-synaptic homeostasis at the myasthenic neuromuscular junction.* Front Biosci (Landmark Ed), 2017. **22**(7): p. 1033-1051.

61. Abd Al Samid, M., et al., *A functional human motor unit platform engineered from human embryonic stem cells and immortalized skeletal myoblasts.* Stem Cells Cloning, 2018. **11**: p. 85-93.
62. Chakkalakal, J.V., et al., *Retrograde influence of muscle fibers on their innervation revealed by a novel marker for slow motoneurons.* Development, 2010. **137**(20): p. 3489-99.
63. Baehr, L.M., et al., *Age-related deficits in skeletal muscle recovery following disuse are associated with neuromuscular junction instability and ER stress, not impaired protein synthesis.* Aging (Albany NY), 2016. **8**(1): p. 127-46.
64. Janssen, I., et al., *Skeletal muscle mass and distribution in 468 men and women aged 18-88 yr.* J Appl Physiol (1985), 2000. **89**(1): p. 81-8.
65. Carlson, B.M., *Factors influencing the repair and adaptation of muscles in aged individuals: satellite cells and innervation.* J Gerontol A Biol Sci Med Sci, 1995. **50 Spec No**: p. 96-100.
66. Nilwik, R., et al., *The decline in skeletal muscle mass with aging is mainly attributed to a reduction in type II muscle fiber size.* Exp Gerontol, 2013. **48**(5): p. 492-8.
67. Andersen, J.L., *Muscle fibre type adaptation in the elderly human muscle.* Scand J Med Sci Sports, 2003. **13**(1): p. 40-7.
68. Larsson, L., G. Grimby, and J. Karlsson, *Muscle strength and speed of movement in relation to age and muscle morphology.* J Appl Physiol Respir Environ Exerc Physiol, 1979. **46**(3): p. 451-6.
69. Wong, S.L., *Grip strength reference values for Canadians aged 6 to 79: Canadian Health Measures Survey, 2007 to 2013.* Health Rep, 2016. **27**(10): p. 3-10.
70. Reid, K.F. and R.A. Fielding, *Skeletal muscle power: a critical determinant of physical functioning in older adults.* Exerc Sport Sci Rev, 2012. **40**(1): p. 4-12.
71. Frontera, W.R., et al., *Aging of skeletal muscle: a 12-yr longitudinal study.* J Appl Physiol (1985), 2000. **88**(4): p. 1321-6.
72. Kemmler, W., et al., *Changes of Maximum Leg Strength Indices During Adulthood a Cross-Sectional Study With Non-athletic Men Aged 19-91.* Front Physiol, 2018. **9**: p. 1524.
73. Bean, J.F., et al., *The relationship between leg power and physical performance in mobility-limited older people.* J Am Geriatr Soc, 2002. **50**(3): p. 461-7.
74. Reid, K.F., et al., *Longitudinal decline of lower extremity muscle power in healthy and mobility-limited older adults: influence of muscle mass, strength, composition, neuromuscular activation and single fiber contractile properties.* Eur J Appl Physiol, 2014. **114**(1): p. 29-39.
75. Skelton, D.A., et al., *Strength, power and related functional ability of healthy people aged 65-89 years.* Age Ageing, 1994. **23**(5): p. 371-7.
76. Aagaard, P., et al., *Mechanical muscle function, morphology, and fiber type in lifelong trained elderly.* Med Sci Sports Exerc, 2007. **39**(11): p. 1989-96.
77. Butikofer, L., et al., *Destabilization of the neuromuscular junction by proteolytic cleavage of agrin results in precocious sarcopenia.* FASEB J, 2011. **25**(12): p. 4378-93.
78. Gutmann, E. and V. Hanzlikova, *Motor unit in old age.* Nature, 1966. **209**(5026): p. 921-2.
79. D'Antona, G., et al., *The effect of ageing and immobilization on structure and function of human skeletal muscle fibres.* J Physiol, 2003. **552**(Pt 2): p. 499-511.

80. Lowe, D.A., et al., *Electron paramagnetic resonance reveals age-related myosin structural changes in rat skeletal muscle fibers.* Am J Physiol Cell Physiol, 2001. **280**(3): p. C540-7.
81. Piasecki, M., et al., *Age-related neuromuscular changes affecting human vastus lateralis.* J Physiol, 2016. **594**(16): p. 4525-36.
82. Lexell, J. and D.Y. Downham, *The occurrence of fibre-type grouping in healthy human muscle: a quantitative study of cross-sections of whole vastus lateralis from men between 15 and 83 years.* Acta Neuropathol, 1991. **81**(4): p. 377-81.
83. Kelly, N.A., et al., *Effects of aging and Parkinson's disease on motor unit remodeling: influence of resistance exercise training.* J Appl Physiol (1985), 2018. **124**(4): p. 888-898.
84. Piasecki, M., et al., *Age-dependent motor unit remodelling in human limb muscles.* Biogerontology, 2016. **17**(3): p. 485-96.
85. McNeil, C.J., et al., *Motor unit number estimates in the tibialis anterior muscle of young, old, and very old men.* Muscle Nerve, 2005. **31**(4): p. 461-7.
86. Piasecki, M., et al., *Failure to expand the motor unit size to compensate for declining motor unit numbers distinguishes sarcopenic from non-sarcopenic older men.* J Physiol, 2018. **596**(9): p. 1627-1637.
87. Manta, P., D. Vassilopoulos, and M. Spengos, *Nucleo-cytoplasmic ratio in ageing skeletal muscle.* Eur Arch Psychiatry Neurol Sci, 1987. **236**(4): p. 235-6.
88. Kadi, F., et al., *Satellite cells and myonuclei in young and elderly women and men.* Muscle Nerve, 2004. **29**(1): p. 120-7.
89. Roth, S.M., et al., *Skeletal muscle satellite cell populations in healthy young and older men and women.* Anat Rec, 2000. **260**(4): p. 351-8.
90. Schultz, E. and B.H. Lipton, *Skeletal muscle satellite cells: changes in proliferation potential as a function of age.* Mech Ageing Dev, 1982. **20**(4): p. 377-83.
91. Ballak, S.B., et al., *Blunted hypertrophic response in old mouse muscle is associated with a lower satellite cell density and is not alleviated by resveratrol.* Exp Gerontol, 2015. **62**: p. 23-31.
92. van Deursen, J.M., *The role of senescent cells in ageing.* Nature, 2014. **509**(7501): p. 439-46.
93. Yousefzadeh, M.J., et al., *Tissue specificity of senescent cell accumulation during physiologic and accelerated aging of mice.* Aging Cell, 2020. **19**(3): p. e13094.
94. Hayflick, L. and P.S. Moorhead, *The serial cultivation of human diploid cell strains.* Exp Cell Res, 1961. **25**: p. 585-621.
95. Hayflick, L., *The Limited in Vitro Lifetime of Human Diploid Cell Strains.* Exp Cell Res, 1965. **37**: p. 614-36.
96. d'Adda di Fagagna, F., *Living on a break: cellular senescence as a DNA-damage response.* Nat Rev Cancer, 2008. **8**(7): p. 512-22.
97. Kuilman, T., et al., *The essence of senescence.* Genes Dev, 2010. **24**(22): p. 2463-79.
98. Basisty, N., et al., *A proteomic atlas of senescence-associated secretomes for aging biomarker development.* PLoS Biol, 2020. **18**(1): p. e3000599.
99. Chikenji, T.S., et al., *p16(INK4A)-expressing mesenchymal stromal cells restore the senescence-clearance-regeneration sequence that is impaired in chronic muscle inflammation.* EBioMedicine, 2019. **44**: p. 86-97.

100. Levi, N., et al., *The ECM path of senescence in aging: components and modifiers.* FEBS J, 2020. **287**(13): p. 2636-2646.
101. Neves, J., et al., *Of flies, mice, and men: evolutionarily conserved tissue damage responses and aging.* Dev Cell, 2015. **32**(1): p. 9-18.
102. von Zglinicki, T., T. Wan, and S. Miwa, *Senescence in Post-Mitotic Cells: A Driver of Aging?* Antioxid Redox Signal, 2021. **34**(4): p. 308-323.
103. Jurk, D., et al., *Postmitotic neurons develop a p21-dependent senescence-like phenotype driven by a DNA damage response.* Aging Cell, 2012. **11**(6): p. 996-1004.
104. Dungan, C.M., et al., *In vivo analysis of gammaH2AX+ cells in skeletal muscle from aged and obese humans.* FASEB J, 2020. **34**(5): p. 7018-7035.
105. Song, S., et al., *Targeting Senescent Cells for a Healthier Aging: Challenges and Opportunities.* Adv Sci (Weinh), 2020. **7**(23): p. 2002611.
106. Baker, D.J., et al., *Naturally occurring p16(Ink4a)-positive cells shorten healthy lifespan.* Nature, 2016. **530**(7589): p. 184-9.
107. Demaria, M., et al., *Cellular Senescence Promotes Adverse Effects of Chemotherapy and Cancer Relapse.* Cancer Discov, 2017. **7**(2): p. 165-176.
108. Calcinotto, A., et al., *Cellular Senescence: Aging, Cancer, and Injury.* Physiol Rev, 2019. **99**(2): p. 1047-1078.
109. Tumasian, R.A., 3rd, et al., *Skeletal muscle transcriptome in healthy aging.* Nat Commun, 2021. **12**(1): p. 2014.
110. Smith, J.R. and O.M. Pereira-Smith, *Replicative senescence: implications for in vivo aging and tumor suppression.* Science, 1996. **273**(5271): p. 63-7.
111. Zhu, Y., et al., *The Achilles' heel of senescent cells: from transcriptome to senolytic drugs.* Aging Cell, 2015. **14**(4): p. 644-58.
112. Xu, M., et al., *Senolytics improve physical function and increase lifespan in old age.* Nat Med, 2018. **24**(8): p. 1246-1256.
113. Dungan, C.M., et al., *Deletion of SA beta-Gal+ cells using senolytics improves muscle regeneration in old mice.* Aging Cell, 2022. **21**(1): p. e13528.
114. Grinnell, A.D. and A.A. Herrera, *Specificity and plasticity of neuromuscular connections: long-term regulation of motoneuron function.* Progress in Neurobiology, 1981. **17**(4): p. 203-282.
115. Sanes, J.R., *More nerve growth factors?* Nature, 1984. **307**(5951): p. 500.
116. Fahim, M.A. and N. Robbins, *Ultrastructural studies of young and old mouse neuromuscular junctions.* J Neurocytol, 1982. **11**(4): p. 641-56.
117. Rosenheimer, J.L., *Factors affecting denervation-like changes at the neuromuscular junction during aging.* Int J Dev Neurosci, 1990. **8**(6): p. 643-54.
118. Courtney, J. and J.H. Steinbach, *Age changes in neuromuscular junction morphology and acetylcholine receptor distribution on rat skeletal muscle fibres.* J Physiol, 1981. **320**: p. 435-47.
119. Valdez, G., et al., *Attenuation of age-related changes in mouse neuromuscular synapses by caloric restriction and exercise.* Proc Natl Acad Sci U S A, 2010. **107**(33): p. 14863-8.
120. Kurokawa, K., et al., *Age-related change in peripheral nerve conduction: compound muscle action potential duration and dispersion.* Gerontology, 1999. **45**(3): p. 168-73.
121. Soendenbroe, C., et al., *Molecular indicators of denervation in aging human skeletal muscle.* Muscle Nerve, 2019. **60**(4): p. 453-463.

122. Urbanchek, M.G., et al., *Specific force deficit in skeletal muscles of old rats is partially explained by the existence of denervated muscle fibers.* J Gerontol A Biol Sci Med Sci, 2001. **56**(5): p. B191-7.
123. Olsen, M., et al., *The ability to re-express polysialylated NCAM in soleus muscle after denervation is reduced in aged rats compared to young adult rats.* Int J Dev Neurosci, 1995. **13**(2): p. 97-104.
124. Kobayashi, H., N. Robbins, and U. Rutishauser, *Neural cell adhesion molecule in aged mouse muscle.* Neuroscience, 1992. **48**(1): p. 237-48.
125. Ye, J., et al., *FBXO40, a gene encoding a novel muscle-specific F-box protein, is upregulated in denervation-related muscle atrophy.* Gene, 2007. **404**(1-2): p. 53-60.
126. Axelsson, J. and S. Thesleff, *A study of supersensitivity in denervated mammalian skeletal muscle.* J Physiol, 1959. **147**(1): p. 178-93.
127. Bhattacharya, A., et al., *Denervation induces cytosolic phospholipase A2-mediated fatty acid hydroperoxide generation by muscle mitochondria.* J Biol Chem, 2009. **284**(1): p. 46-55.
128. Wang, Z.M., et al., *Extension and magnitude of denervation in skeletal muscle from ageing mice.* J Physiol, 2005. **565**(Pt 3): p. 757-64.
129. Rowan, S.L., et al., *Denervation causes fiber atrophy and myosin heavy chain co-expression in senescent skeletal muscle.* PLoS One, 2012. **7**(1): p. e29082.
130. Schiaffino, S., et al., *Embryonic and neonatal myosin heavy chain in denervated and paralyzed rat skeletal muscle.* Dev Biol, 1988. **127**(1): p. 1-11.
131. Capkovic, K.L., et al., *Neural cell adhesion molecule (NCAM) marks adult myogenic cells committed to differentiation.* Exp Cell Res, 2008. **314**(7): p. 1553-65.
132. Cashman, N.R., et al., *Neural cell adhesion molecule in normal, denervated, and myopathic human muscle.* Ann Neurol, 1987. **21**(5): p. 481-9.
133. Fidzianska, A. and A. Kaminska, *Neural cell adhesion molecule (N-CAM) as a marker of muscle tissue alternations. Review of the literature and own observations.* Folia Neuropathol, 1995. **33**(3): p. 125-8.
134. Covault, J. and J.R. Sanes, *Distribution of N-CAM in synaptic and extrasynaptic portions of developing and adult skeletal muscle.* J Cell Biol, 1986. **102**(3): p. 716-30.
135. Illa, I., M. Leon-Monzon, and M.C. Dalakas, *Regenerating and denervated human muscle fibers and satellite cells express neural cell adhesion molecule recognized by monoclonal antibodies to natural killer cells.* Ann Neurol, 1992. **31**(1): p. 46-52.
136. Covault, J. and J.R. Sanes, *Neural cell adhesion molecule (N-CAM) accumulates in denervated and paralyzed skeletal muscles.* Proc Natl Acad Sci U S A, 1985. **82**(13): p. 4544-8.
137. Reyes, A.A., S.J. Small, and R. Akeson, *At least 27 alternatively spliced forms of the neural cell adhesion molecule mRNA are expressed during rat heart development.* Mol Cell Biol, 1991. **11**(3): p. 1654-61.
138. Soroka, V., et al., *Structure and interactions of NCAM Ig1-2-3 suggest a novel zipper mechanism for homophilic adhesion.* Structure, 2003. **11**(10): p. 1291-301.
139. Walmod, P.S., et al., *Zippers make signals: NCAM-mediated molecular interactions and signal transduction.* Neurochem Res, 2004. **29**(11): p. 2015-35.
140. Daniloff, J.K., et al., *Altered expression of neuronal cell adhesion molecules induced by nerve injury and repair.* J Cell Biol, 1986. **103**(3): p. 929-45.

141. Moore, S.E. and F.S. Walsh, *Nerve dependent regulation of neural cell adhesion molecule expression in skeletal muscle.* Neuroscience, 1986. **18**(2): p. 499-505.
142. Mosole, S., et al., *Long-term high-level exercise promotes muscle reinnervation with age.* J Neuropathol Exp Neurol, 2014. **73**(4): p. 284-94.
143. Gillon, A. and P. Sheard, *Elderly mouse skeletal muscle fibres have a diminished capacity to upregulate NCAM production in response to denervation.* Biogerontology, 2015. **16**(6): p. 811-23.
144. Gundersen, K., et al., *Overexpression of myogenin in muscles of transgenic mice: interaction with Id-1, negative crossregulation of myogenic factors, and induction of extrasynaptic acetylcholine receptor expression.* Mol Cell Biol, 1995. **15**(12): p. 7127-34.
145. Merlie, J.P. and J.R. Sanes, *Concentration of acetylcholine receptor mRNA in synaptic regions of adult muscle fibres.* Nature, 1985. **317**(6032): p. 66-8.
146. Goldman, D. and J. Staple, *Spatial and temporal expression of acetylcholine receptor RNAs in innervated and denervated rat soleus muscle.* Neuron, 1989. **3**(2): p. 219-28.
147. Macpherson, P.C., X. Wang, and D. Goldman, *Myogenin regulates denervation-dependent muscle atrophy in mouse soleus muscle.* J Cell Biochem, 2011. **112**(8): p. 2149-59.
148. Duclert, A., J. Piette, and J.P. Changeux, *Influence of innervation of myogenic factors and acetylcholine receptor alpha-subunit mRNAs.* Neuroreport, 1991. **2**(1): p. 25-8.
149. Merlie, J.P., et al., *Myogenin and acetylcholine receptor alpha gene promoters mediate transcriptional regulation in response to motor innervation.* J Biol Chem, 1994. **269**(4): p. 2461-7.
150. Gilmour, B.P., et al., *Multiple binding sites for myogenic regulatory factors are required for expression of the acetylcholine receptor gamma-subunit gene.* J Biol Chem, 1991. **266**(30): p. 19871-4.
151. Prody, C.A. and J.P. Merlie, *A developmental and tissue-specific enhancer in the mouse skeletal muscle acetylcholine receptor alpha-subunit gene regulated by myogenic factors.* J Biol Chem, 1991. **266**(33): p. 22588-96.
152. Pestronk, A. and D.B. Drachman, *Motor nerve sprouting and acetylcholine receptors.* Science, 1978. **199**(4334): p. 1223-5.
153. Fontaine, B., et al., *Detection of the nicotinic acetylcholine receptor alpha-subunit mRNA by in situ hybridization at neuromuscular junctions of 15-day-old chick striated muscles.* EMBO J, 1988. **7**(3): p. 603-9.
154. Tsay, H.J. and J. Schmidt, *Skeletal muscle denervation activates acetylcholine receptor genes.* J Cell Biol, 1989. **108**(4): p. 1523-6.
155. Goldman, D., H.R. Brenner, and S. Heinemann, *Acetylcholine receptor alpha-, beta-, gamma-, and delta-subunit mRNA levels are regulated by muscle activity.* Neuron, 1988. **1**(4): p. 329-33.
156. Goldman, D., et al., *Muscle denervation increases the levels of two mRNAs coding for the acetylcholine receptor alpha-subunit.* J Neurosci, 1985. **5**(9): p. 2553-8.
157. Miledi, R., *The acetylcholine sensitivity of frog muscle fibres after complete or partial devervation.* J Physiol, 1960. **151**(1): p. 1-23.
158. Westcott, W.L., *Resistance training is medicine: effects of strength training on health.* Curr Sports Med Rep, 2012. **11**(4): p. 209-16.

159. Hakkinen, K., et al., *Changes in muscle morphology, electromyographic activity, and force production characteristics during progressive strength training in young and older men.* J Gerontol A Biol Sci Med Sci, 1998. **53**(6): p. B415-23.
160. Ruple, B.A., et al., *Resistance training rejuvenates the mitochondrial methylome in aged human skeletal muscle.* FASEB J, 2021. **35**(9): p. e21864.
161. Newton, R.U., et al., *Mixed-methods resistance training increases power and strength of young and older men.* Med Sci Sports Exerc, 2002. **34**(8): p. 1367-75.
162. Hakkinen, K., et al., *Changes in electromyographic activity, muscle fibre and force production characteristics during heavy resistance/power strength training in middle-aged and older men and women.* Acta Physiol Scand, 2001. **171**(1): p. 51-62.
163. Jozsi, A.C., et al., *Changes in power with resistance training in older and younger men and women.* J Gerontol A Biol Sci Med Sci, 1999. **54**(11): p. M591-6.
164. Welle, S., S. Totterman, and C. Thornton, *Effect of age on muscle hypertrophy induced by resistance training.* J Gerontol A Biol Sci Med Sci, 1996. **51**(6): p. M270-5.
165. Lee, J.D., et al., *Aged Muscle Demonstrates Fiber-Type Adaptations in Response to Mechanical Overload, in the Absence of Myofiber Hypertrophy, Independent of Satellite Cell Abundance.* J Gerontol A Biol Sci Med Sci, 2016. **71**(4): p. 461-7.
166. Raue, U., et al., *Improvements in whole muscle and myocellular function are limited with high-intensity resistance training in octogenarian women.* J Appl Physiol (1985), 2009. **106**(5): p. 1611-7.
167. Frontera, W.R., et al., *Strength training in older women: early and late changes in whole muscle and single cells.* Muscle Nerve, 2003. **28**(5): p. 601-8.
168. Miller, M.S., et al., *Moderate-intensity resistance exercise alters skeletal muscle molecular and cellular structure and function in inactive older adults with knee osteoarthritis.* J Appl Physiol (1985), 2017. **122**(4): p. 775-787.
169. Dankel, S.J., et al., *Resistance training induced changes in strength and specific force at the fiber and whole muscle level: a meta-analysis.* Eur J Appl Physiol, 2019. **119**(1): p. 265-278.
170. Proud, C.G., *mTORC1 signalling and mRNA translation.* Biochem Soc Trans, 2009. **37**(Pt 1): p. 227-31.
171. Bodine, S.C., et al., *Akt/mTOR pathway is a crucial regulator of skeletal muscle hypertrophy and can prevent muscle atrophy in vivo.* Nat Cell Biol, 2001. **3**(11): p. 1014-9.
172. Fry, C.S., et al., *Aging impairs contraction-induced human skeletal muscle mTORC1 signaling and protein synthesis.* Skelet Muscle, 2011. **1**(1): p. 11.
173. Welle, S., C. Thornton, and M. Statt, *Myofibrillar protein synthesis in young and old human subjects after three months of resistance training.* Am J Physiol, 1995. **268**(3 Pt 1): p. E422-7.
174. Toth, M.J., et al., *Age-related differences in skeletal muscle protein synthesis: relation to markers of immune activation.* Am J Physiol Endocrinol Metab, 2005. **288**(5): p. E883-91.
175. Balagopal, P., et al., *Effects of aging on in vivo synthesis of skeletal muscle myosin heavy-chain and sarcoplasmic protein in humans.* Am J Physiol, 1997. **273**(4): p. E790-800.
176. Yarasheski, K.E., J.J. Zachwieja, and D.M. Bier, *Acute effects of resistance exercise on muscle protein synthesis rate in young and elderly men and women.* Am J Physiol, 1993. **265**(2 Pt 1): p. E210-4.

177. Dorrens, J. and M.J. Rennie, *Effects of ageing and human whole body and muscle protein turnover.* Scand J Med Sci Sports, 2003. **13**(1): p. 26-33.
178. Wall, B.T., et al., *Aging Is Accompanied by a Blunted Muscle Protein Synthetic Response to Protein Ingestion.* PLoS One, 2015. **10**(11): p. e0140903.
179. Drummond, M.J., et al., *Skeletal muscle protein anabolic response to resistance exercise and essential amino acids is delayed with aging.* J Appl Physiol (1985), 2008. **104**(5): p. 1452-61.
180. Raue, U., et al., *Transcriptome signature of resistance exercise adaptations: mixed muscle and fiber type specific profiles in young and old adults.* J Appl Physiol (1985), 2012. **112**(10): p. 1625-36.
181. Voisin, S., et al., *Meta-analysis of genome-wide DNA methylation and integrative omics of age in human skeletal muscle.* J Cachexia Sarcopenia Muscle, 2021. **12**(4): p. 1064-1078.
182. Bird, A., *DNA methylation patterns and epigenetic memory.* Genes Dev, 2002. **16**(1): p. 6-21.
183. Rowlands, D.S., et al., *Multi-omic integrated networks connect DNA methylation and miRNA with skeletal muscle plasticity to chronic exercise in Type 2 diabetic obesity.* Physiol Genomics, 2014. **46**(20): p. 747-65.
184. Dimauro, I., et al., *Resistance training and redox homeostasis: Correlation with age-associated genomic changes.* Redox Biol, 2016. **10**: p. 34-44.
185. Seaborne, R.A., et al., *Methylome of human skeletal muscle after acute & chronic resistance exercise training, detraining & retraining.* Sci Data, 2018. **5**: p. 180213.
186. Grimby, G., et al., *Training can improve muscle strength and endurance in 78- to 84-yr-old men.* J Appl Physiol (1985), 1992. **73**(6): p. 2517-23.
187. Slivka, D., et al., *Single muscle fiber adaptations to resistance training in old (>80 yr) men: evidence for limited skeletal muscle plasticity.* Am J Physiol Regul Integr Comp Physiol, 2008. **295**(1): p. R273-80.
188. Mero, A.A., et al., *Resistance training induced increase in muscle fiber size in young and older men.* Eur J Appl Physiol, 2013. **113**(3): p. 641-50.
189. Barry, B.K., G.E. Warman, and R.G. Carson, *Age-related differences in rapid muscle activation after rate of force development training of the elbow flexors.* Exp Brain Res, 2005. **162**(1): p. 122-32.
190. Kamen, G. and C.A. Knight, *Training-related adaptations in motor unit discharge rate in young and older adults.* J Gerontol A Biol Sci Med Sci, 2004. **59**(12): p. 1334-8.
191. Power, G.A., et al., *Motor unit number estimates in masters runners: use it or lose it?* Med Sci Sports Exerc, 2010. **42**(9): p. 1644-50.
192. Sexton, C.L., et al., *Effects of Peanut Protein Supplementation on Resistance Training Adaptations in Younger Adults.* Nutrients, 2021. **13**(11).
193. Ruple, B.A., et al., *Myofibril and Mitochondrial Area Changes in Type I and II Fibers Following 10 Weeks of Resistance Training in Previously Untrained Men.* Front Physiol, 2021. **12**: p. 728683.
194. Casa, D.J., et al., *National athletic trainers' association position statement: fluid replacement for athletes.* J Athl Train, 2000. **35**(2): p. 212-24.
195. Ruple, B.A., et al., *Comparisons between skeletal muscle imaging techniques and histology in tracking midthigh hypertrophic adaptations following 10 weeks of resistance training.* J Appl Physiol (1985), 2022.

196. Roberts, M.D., et al., *An optimized procedure for isolation of rodent and human skeletal muscle sarcoplasmic and myofibrillar proteins.* J Biol Methods, 2020. **7**(1): p. e127.
197. Blume, J.E., et al., *Rapid, deep and precise profiling of the plasma proteome with multi-nanoparticle protein corona.* Nat Commun, 2020. **11**(1): p. 3662.
198. Zykovich, A., et al., *Genome-wide DNA methylation changes with age in disease-free human skeletal muscle.* Aging Cell, 2014. **13**(2): p. 360-6.
199. The Gene Ontology, C., *The Gene Ontology Resource: 20 years and still GOing strong.* Nucleic Acids Res, 2019. **47**(D1): p. D330-D338.
200. UniProt, C., *UniProt: a hub for protein information.* Nucleic Acids Res, 2015. **43**(Database issue): p. D204-12.
201. Wen, Y., et al., *MyoVision: software for automated high-content analysis of skeletal muscle immunohistochemistry.* J Appl Physiol (1985), 2018. **124**(1): p. 40-51.
202. Zou, K.H., K. Tuncali, and S.G. Silverman, *Correlation and simple linear regression.* Radiology, 2003. **227**(3): p. 617-22.
203. Zhang, X., et al., *Characterization of cellular senescence in aging skeletal muscle.* Nat Aging, 2022. **2**(7): p. 601-615.
204. Englund, D.A., et al., *Skeletal muscle aging, cellular senescence, and senotherapeutics: Current knowledge and future directions.* Mech Ageing Dev, 2021. **200**: p. 111595.
205. Baar, M.P., et al., *Musculoskeletal senescence: a moving target ready to be eliminated.* Curr Opin Pharmacol, 2018. **40**: p. 147-155.
206. Lamb, D.A., et al., *Resistance training increases muscle NAD(+) and NADH concentrations as well as NAMPT protein levels and global sirtuin activity in middle-aged, overweight, untrained individuals.* Aging (Albany NY), 2020. **12**(10): p. 9447-9460.
207. Roberts, M., et al., *A novel deep proteomic approach in human skeletal muscle unveils distinct molecular signatures affected by aging and resistance training.* bioRxiv, 2023: p. 2023.06.02.543459.
208. Mi, H., et al., *Large-scale gene function analysis with the PANTHER classification system.* Nat Protoc, 2013. **8**(8): p. 1551-66.
209. Mi, H., et al., *Protocol Update for large-scale genome and gene function analysis with the PANTHER classification system (v.14.0).* Nat Protoc, 2019. **14**(3): p. 703-721.
210. Kuilman, T. and D.S. Peeper, *Senescence-messaging secretome: SMS-ing cellular stress.* Nat Rev Cancer, 2009. **9**(2): p. 81-94.
211. Faget, D.V., Q. Ren, and S.A. Stewart, *Unmasking senescence: context-dependent effects of SASP in cancer.* Nat Rev Cancer, 2019. **19**(8): p. 439-453.
212. Chen, X.K., et al., *Is exercise a senolytic medicine? A systematic review.* Aging Cell, 2021. **20**(1): p. e13294.
213. Zhang, X., et al., *Exercise Counters the Age-Related Accumulation of Senescent Cells.* Exerc Sport Sci Rev, 2022. **50**(4): p. 213-221.
214. Yang, C., et al., *Aged cells in human skeletal muscle after resistance exercise.* Aging (Albany NY), 2018. **10**(6): p. 1356-1365.
215. Englund, D.A., et al., *Exercise reduces circulating biomarkers of cellular senescence in humans.* Aging Cell, 2021. **20**(7): p. e13415.
216. Justice, J.N., et al., *Cellular Senescence Biomarker p16INK4a+ Cell Burden in Thigh Adipose is Associated With Poor Physical Function in Older Women.* J Gerontol A Biol Sci Med Sci, 2018. **73**(7): p. 939-945.

217. Wu, J., et al., *Ginsenoside Rg1 supplementation clears senescence-associated beta-galactosidase in exercising human skeletal muscle.* J Ginseng Res, 2019. **43**(4): p. 580-588.
218. Wong, W., et al., *The exercise cytokine interleukin-15 rescues slow wound healing in aged mice.* J Biol Chem, 2019. **294**(52): p. 20024-20038.
219. Saito, Y., et al., *Exercise enhances skeletal muscle regeneration by promoting senescence in fibro-adipogenic progenitors.* Nat Commun, 2020. **11**(1): p. 889.
220. Kadi, F., et al., *Cellular adaptation of the trapezius muscle in strength-trained athletes.* Histochem Cell Biol, 1999. **111**(3): p. 189-95.
221. Mackey, A.L., et al., *Enhanced satellite cell proliferation with resistance training in elderly men and women.* Scand J Med Sci Sports, 2007. **17**(1): p. 34-42.
222. Verdijk, L.B., et al., *Skeletal muscle hypertrophy following resistance training is accompanied by a fiber type-specific increase in satellite cell content in elderly men.* J Gerontol A Biol Sci Med Sci, 2009. **64**(3): p. 332-9.
223. Petrella, J.K., et al., *Potent myofiber hypertrophy during resistance training in humans is associated with satellite cell-mediated myonuclear addition: a cluster analysis.* J Appl Physiol (1985), 2008. **104**(6): p. 1736-42.
224. Mackey, A.L., et al., *Differential satellite cell density of type I and II fibres with lifelong endurance running in old men.* Acta Physiol (Oxf), 2014. **210**(3): p. 612-27.
225. Fry, C.S., et al., *Myogenic Progenitor Cells Control Extracellular Matrix Production by Fibroblasts during Skeletal Muscle Hypertrophy.* Cell Stem Cell, 2017. **20**(1): p. 56-69.
226. Fry, C.S., et al., *Regulation of the muscle fiber microenvironment by activated satellite cells during hypertrophy.* FASEB J, 2014. **28**(4): p. 1654-65.
227. Ruple, B.A., et al., *Changes in vastus lateralis fibre cross-sectional area, pennation angle and fascicle length do not predict changes in muscle cross-sectional area.* Exp Physiol, 2022. **107**(11): p. 1216-1224.